Review
Effects of environment and temperature on ceramic tensile strength–grain size relations

R. W. RICE
5411 Hopark Drive, Alexandria, VA, 22310, USA

Overall strength (σ)–grain size (G), i.e. σ–$G^{-1/2}$, relations retain the same basic two-branched character to at least 1200–1300 °C. However, some polycrystalline as well as single crystal strength shifts or deviations are seen relative to each other, and especially relative to Young's moduli versus temperature for poly- and single crystals. The variety and complexity of these deviations are illustrated mainly by Al_2O_3, BeO, MgO and ZrO_2 for which there is considerable data. At ~22 °C, Al_2O_3 polycrystals show substantial strength decrease due to H_2O while MgO, ZrO_2 and BeO polycrystals have limited, variable decreases. Al_2O_3 single crystals (sapphire) also show substantial strength decreases, but ZrO_2 and MgO single crystals show little or none. Sapphire's strength markedly decreases from at least −196 °C to a minimum in the 400–600 °C range, then rises to a maximum at ⩾1000 °C, followed by an accelerating decrease with further temperature increase. Polycrystalline Al_2O_3 shows similar (but less pronounced) strength minima and maxima, or alternatively an approximate strength plateau from ~22 to ~1000 °C interrupting the normally expected strength decreases with increasing temperature at suitably large grain size and absence of defects (e.g. pores) dominating failure. BeO crystals show a linear strength decrease with increasing temperature (T) similar to that of Young's modulus. BeO polycrystals often show a significant strength (apparently grain size and impurity dependent) maximum (at ~500–800 °C) or plateau (from ~22 to ~1000 °C) interrupting an otherwise continuous decrease. MgO shows similar temperature behaviour to BeO, but more pronounced crystal strength decrease and less pronounced polycrystalline strength maxima. Polycrystalline ZrO_2 shows more rapid Young's modulus (E), and especially strength, decreases at ~200–500 °C than single crystals. More limited data for other materials also shows greater, variable σ–T versus E–T trends, e.g. $MgAl_2O_4$ has a similar, but less pronounced decrease than ZrO_2. Collectively these deviations suggest variable impacts on primarily flaw controlled σ–$G^{-1/2}$ behaviour due to factors such as microplasticity, machining stresses, and thermal expansion and elastic anisotropies requiring more comprehensive testing and evaluation to better sort out these effects.

1. Introduction

This paper reviews effects of test environment and (mainly moderate) temperature on the flexure strength (σ) of polycrystalline ceramics as a function of grain size (G). Addition insight is sought by comparing these trends with the behaviour of single crystals (where available) and of Young's modulus. This paper compliments other reviews of σ–$G^{-1/2}$ behaviour at 22 °C, updating and extending them [1–4], particularly with regard to environmental and temperature effects. The purpose of this paper is to consider these factors as a guide to better understand mechanisms operative at or near 22 °C, especially grain size effects on strength. Thus, while some behaviour in the 1000–1500 °C range is noted, the focus is on the −200 to 1000 °C range; data reflecting substantial creep and high-temperature stress rupture is not considered. Similarly, while environmental effects are considered, the focus is on their impact on σ–G relations. While useful information and implications regarding σ–G relations are obtained, uncertainties and inadequacies are shown, hence providing guidance for improved studies.

2. Strength–grain size–temperature–environment data survey

2.1. Al_2O_3

Overall strength data for Al_2O_3 at −196 °C versus 22 °C [1–10] (Fig. 1) shows: (1) the same two branch σ–$G^{-1/2}$ behaviour, (2) both with finer grain size σ–$G^{-1/2}$ slopes > 0, (3) single crystal strengths > many polycrystalline samples with similar surface finishing, [1–4], and (4) greater single- and poly-crystal

0022–2461

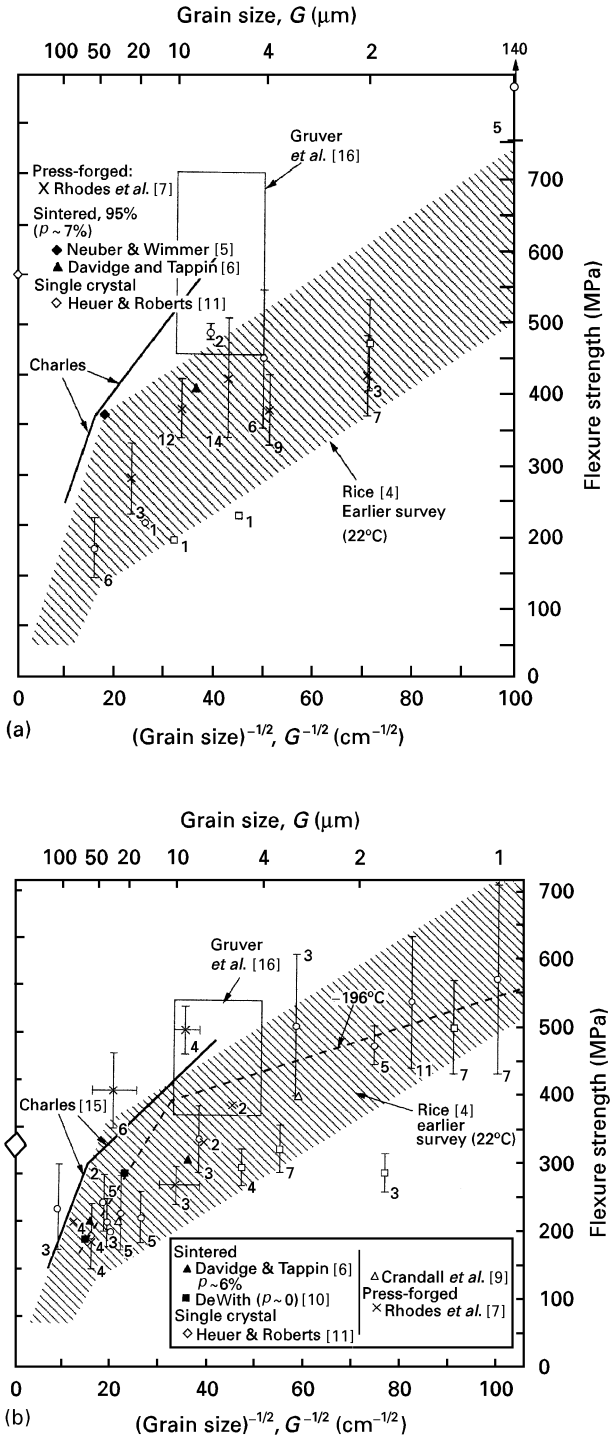

Figure 1 Comparison of σ–$G^{-1/2}$ data, mainly for hot-pressed and pressed forged, Al_2O_3, at -196 and 22 °C. (a) Data at -196 °C (for reference, the range of data from an earlier survey [1] of data at 22 °C is shown). (b) Data at 22 °C (for reference, the mean trend line for actual data at -196 °C from (a) is shown). Note the: (1) generally lower strengths of the authors' specimens made from Linde B (□) versus Linde A (○) powders; (2) possible lower strength level of the pressed forged versus hot-pressed Al_2O_3 at finer G (~10 μm) and the greater scatter of the pressed forged material; (3) single crystal strengths being higher than much of the polycrystalline data at -196 and 22 °C, and direct comparison of Charles [15] and Gruver *et al.*'s [16] data at both temperatures.

strengths at -196 °C versus 22 °C. While some data, e.g. for press forged Al_2O_3 [7], does not clearly show increases at -196 °C versus 22 °C due to scatter and the limited extent of the data, specific comparisons more clearly show single- and poly-crystal strength increases. Thus, Heuer and Roberts [11, 12] showed sapphire strength increasing ~35–50% in liquid N_2 (-196 °C) versus 22 °C in air for various surface finishes. Other investigators [13, 14] showed similar increases but Charles [15] showed a 75% increase. For dense hot pressed Al_2O_3 tested at -196 °C, Rice [3] showed a 30% strength increase for most grain sizes, but a 45% increase for $G = 1$–2 μm. Similarly, Charles [15] showed ~20% strength increase for lamp envelope Al_2O_3 (G~6–150 μm), Neuber and Wimmer [5] a ~30% increase for 99.5% Al_2O_3 (porosity (P) ~5%, G~35 μm), Davidge and Tappin [6] a ~25% strength increase for 95% Al_2O_3, P~7%, G~8 μm, and Gruver *et al.* [16] a ~30% increase for 96% Al_2O_3, P~5%, G~7 μm (Fig. 1a) in liquid N_2 versus air at 22 °C. Overall the polycrystalline strength increase is probably less than for sapphire (except possibly at G~1–2 μm), reinforcing indications of sapphire strengths being even > many polycrystalline values at -196 °C versus 22 °C. Tests in the absence of H_2O at 22 °C (e.g. in vacuum) showed much, but not all, of the increase in strength at -196 °C is due to the elimination of slow crack growth (SCG). Thus, Charles showed sapphire strength increased only ~17% at -196 versus 22 °C, but decreased ~50% in wet air versus vacuum at 22 °C, while lamp envelope Al_2O_3 (G~40 μm) showed only about 8% increase, and ~44% decrease respectively; i.e. indicating less increase in liquid N_2, but similar decrease in wet air to those of sapphire. He also showed ~20% increase in 22 °C (air) strength for a substantial grain size range (G~6–150 μm) at a strain rate of 2.7×10^{-4} versus 1.4×10^{-2} min^{-1}.

McMahon [17] showed strength of sintered, high Al_2O_3 bars at 22 °C being a function only of surface finish and relative humidity (to 70%) during the test, and not of prior humidity exposure. He showed the relative level of strength and its decrease due to H_2O varies as follows for different specimen surface conditions: (1) as-fired surfaces gave the lowest strength and the least (~5%) strength decrease, (2) surfaces ground perpendicular to the specimen axis gave intermediate strengths and the greatest (~15%) decrease, and (3) surfaces ground parallel with the specimen length gave the highest strength and an intermediate strength decrease with increasing relative humidity. Thus, the relative strength decrease with increasing humidity was a function of surface finish as well as moisture content. Rice [4] showed that dense, hot-pressed Al_2O_3 averaged ~20% strength decrease on testing in distilled H_2O versus air at 22 °C, but that re-testing in air bar sections previously tested in H_2O (after drying) returned them to their original air strength. These two studies show strength degradation due to SCG occurs only during actual loading and is a function of the environment only during stressing. This implies that SCG either does not occur due to microstructural (e.g. thermal expansion anisotropy, TEA) stresses or that it saturates (at least for typical multi-grain size flaws) after initial exposure. Significant decreases in Young's modulus and internal friction increases of HfO_2 [18] occurred upon opening the vacuum furnace (after sintering or heat treating for grain growth), saturating

after only ~2 days; thus indicated SCG microcracking saturated in the absence of an applied stress.

Increasing temperatures above 22 °C in air generally decreased sapphire strength [12–16, 19–24], often drastically, e.g. losing 1/3 to 3/4 of its strength at 22 °C upon reaching a minimum at 400–600 °C depending on orientation, surface finish, and test environment (see Fig. 4). Hurley [22] observed a rapid strength decrease from 22 to ~400 °C for both $\langle 1\,1\,\bar{2}\,0\rangle$, and C axis ($\langle 0\,0\,0\,1\rangle$) filaments, then a plateau to ~700 and 900 °C respectively before rapidly decreasing again. (However, compression testing of sapphire rods of the same orientations showed respectively a slow decrease, similar to that for Young's modulus, then a very rapid decrease starting at ~800 °C.) The level and, especially the temperature, of the strength minimum can be effected by other parameters. Charles [15] showed the strength minimum at ~900 °C for sapphire tested in air as-annealed (1200 °C) versus 400–600 °C for mechanically finished surfaces. These tests in various atmospheres showed sapphire strength decreasing by ~15% to a minimum at ~600 °C in vacuum with less decrease in dry or wet H_2 (but strength ~20% lower in dry H_2 than in vacuum and ~20% lower for wet versus dry H_2), before all merging together at ~900 °C. Iwasa and Bradt's [23] (indentation-fracture) fracture toughness (K_{IC}) tests of sapphire oriented for basal or rhombohedral fracture showed similar trends; i.e. decreasing ~25 and 75% to minima at ~800 and 1000 °C respectively (see Fig. 4). (Their K_{IC} tests of sapphire oriented for fracture on A or M planes follow the decreases of Young's moduli with increasing temperature). Less strength decrease, i.e. a higher minimum strength (but at a somewhat lower temperature) is indicated in one [16], but not another [14] test of Cr doped sapphire. However, Sayir [24], who observed strength minima at 300 °C and maxima at 900 °C in undoped sapphire, reported that 500 p.p.m. MgO or TiO_2 (separately or combined) doping eliminated the minima and maxima.

Carniglia's survey's [25, 26] of the σ–$G^{-1/2}$ behaviour of Al_2O_3 showed strengths of finer grain size, dense bodies at 400 °C ~ the same as at 22 °C, then decreasing at a moderate rate up to 1000–1200 °C, and more rapidly beyond 1200 °C. Differentiation of strength as a function of temperature in the larger grain size region was even more moderate. (Correcting for Carniglia's failure to plot all data at 22 °C and erroneously plotting some data at higher strength reduces the limited differentiation his plot showed between fine grain bodies at 22 and 400 °C.) Charles' [15] testing of lamp envelope Al_2O_3 (G~40 μm) showed strength approximately constant from ~200–600 °C, then dropping gradually (e.g. ~5%/100 °C) in vacuum, while tests in dry and wet H_2 (the latter again at lower strength levels as for sapphire) showed a strength minima at ~400 °C, and a maxima at ~1100 °C. Neuber and Wimmer's [6] air testing of $a \geqslant 99.5\%$ Al_2O_3 porosity (P) ~5%, G~35 μm) showed distinct strength minima (at ~400 °C), and maxima (at ~800 °C, see Fig. 4) for each of four sets of rods having diameters of 2–8 mm, with the strength levels slightly lower for each increase in diameter. Kirchner *et al.* [27, 28] also showed a definite strength minimum at ~400 °C for their dense hot-pressed Al_2O_3, tested as-polished, or strengthened by surface compression from quenching in silicone oil. The quenched material also showed a strength maximum at ~800 °C; however, there was substantial scatter in both the maxima and minima for their bodies. While Jackman and Roberts' [19] clearly showed such maxima and minima for single crystals, their tests of a 99.3 + % Al_2O_3 (P~5%, G~50 μm) showed only an uncertain indication of a strength minimum at ~500 °C. Mizuta *et al.*'s [29] Hot isostatically pressed HIPed, transparent Al_2O_3 (uniform G~1–2 μm) showed no maxima or minima, instead strength was ~constant at ~780 MPa to > 1000 °C, then dropped to ~700 MPa at 1100 °C. Thus such minima, maxima, or both, or a plateau at intermediate temperatures are shown in almost [4, 11, 12, 14, 30] (Fig. 2), but not [16, 29], all Al_2O_3 studies.

Al_2O_3 σ–$G^{-1/2}$ data [6–11, 31–32] at 1200–1315 °C (Fig. 2) shows two branch behaviour similar to, but with lower strength (e.g. ~50%, possibly more at fine grain size) than at 22 °C (Fig. 1), with reasonable agreement between different studies. Again, higher single crystal than many polycrystalline strengths are seen, as is a σ–$G^{-1/2}$ slope > 0 at finer grain size. While strength–temperature data for bodies of various grain size shows the overall expected strength decrease with increasing grain size, there is commonly a limited maximum, or at least approximately a strength plateau over a significant intermediate temperature range (Fig. 3).

Impurities or additives may or may not have significant effects in this temperature range. Thus, there was no effect of AlON additions (other than via grain size) on strength (or K_{IC}) to at least 800 °C [34], nor of CaO

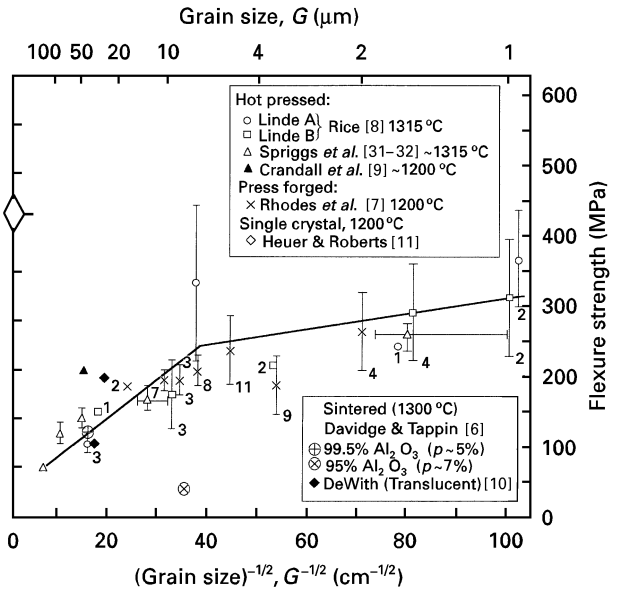

Figure 2 σ–$G^{-1/2}$ data, mainly for hot-pressed and pressed forged Al_2O_3, at 1200–1315 °C. Note the general consistency of data from different sources and its indication of a two-branched σ–$G^{-1/2}$ relationship with the finer G branch having a definite positive slope, and the generally lower strengths relative to those for single crystals.

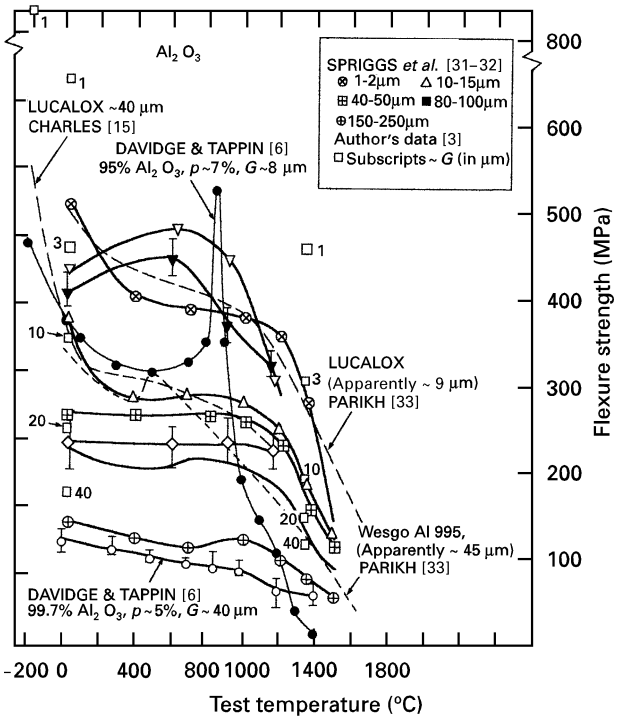

Figure 3 Flexure strength versus test temperature for different Al_2O_3 bodies reflecting primarily different grain sizes and secondarily some composition and processing differences. Note the solid symbol of Crandall *et al.* [9] ($\triangledown$, $\blacktriangledown$, 3 μm, $\diamond$20 μm) is for Al_2O_3 + SiO_2 and the open symbol for pure Al_2O_3, as is all other data except that of McLaren and Davidge [30].

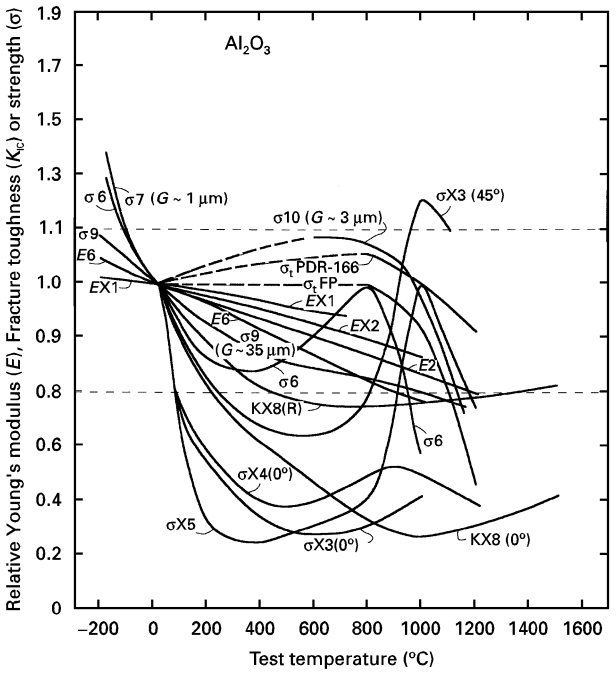

Figure 4 Relative Young's modulus (E) , fracture toughness (K_{IC}), and strength (σ) of single and polycrystalline Al_2O_3 versus test temperature (normalized by taking the property value at 22 °C = 1). X following the property designation (E, K_{IC} and σ) designates single crystal values (followed by the crystal orientation in ( ) if known). Numbers following the property and crystal designations designate the source of the data (from listing, upper right). For polycrystalline values, grain sizes are shown in ( ) where pertinent and available. Curves designated σ_t are for true tensile testing of fibres (FP = a coarser-grained, pure alumina and PDR = a finer-grained alumina–zirconia fibre). While most tests were in air, some were in vacuum or liquid N_2. Note the change in scale between relative values of 0.8 and 1.1 in order to better differentiate the data there, and that E–T trends, especially for single crystals are a key basis of comparison. 1, Wachtman *et al.* [38]; 2, Wachtman & Lam [39]; 3, Wachtman & Maxwell [13]; 4, Shatinian [20]; 5, Heuer & Roberts [11]; 6, Neuber & Wimmer [5]; 7, Rice [3]; 8, Iwasa & Bradt [23]; 9, Charles [15]; 10, Crandall *et al.* [9].

[10], Crandall *et al.* [9] showed similar trends for Al_2O_3 hot pressed with or without 3% SiO_2 (Fig. 3). However, typical commercial (sintered) Al_2O_3 having a SiO_2-based (usually) glass phase commonly show an intermediate (strain rate, composition, and possibly P dependent) strength maxima at 700–1100 °C, then greater strength decreases [7, 30] at higher temperature (Fig. 3).

Al_2O_3 based polycrystalline fibres show similar strength–temperature trends. Tests of pure α-Al_2O_3 (Dupont FP) and Al_2O_3–SiO_2 fibres show the same strengths at 22 and 800 °C, only moderate ($\sim$10%) decrease by 1000 °C, then a more rapid decrease [35–37] (Fig. 4). Al_2O_3–20% ZrO_2 fibres show $\sim$10% higher strength at 800 °C before dropping back to the same strength of 22 °C at $\sim$1000 °C (and more rapid decrease at higher temperatures [35–37]. Neither set of fibres were tested at 22 °C $< T >$ 800 °C.)

The above strength changes with increasing temperature (T) are put in broader perspective by comparing single- and poly-crystal Al_2O_3 (including fibre) strength normalized by their values at 22 °C, along with similar Young's modulus (E) and K_{IC} normalization (Fig. 4). This shows the well known steady E–T decrease of 10–20% for both single- and poly-crystals by 1200 °C [38–40]. This is in marked contrast to a typically much faster initial decrease of both relative crystal K_{IC} and strength (typically oriented for basal or rhombohedral fracture), toward minima at $\sim$400–800 °C, then rising to pronounced strength maxima (that can be greater than that at 22 °C) and then falling (rapidly). While absolute strength values vary as expected (e.g. with surface finish), these trends occur for crystals of various orientations [11, 13, 19] and machining [12, 13], as well as as-grown (0 °C) crystal filaments [20]. Again, while sapphire strength values are higher when H_2O is not present, or with reduced activity, the trends are also relatively independent of the environment since the basic trends are similar, whether the testing is done in vacuum or in air. Most polycrystalline tests at $T >$ 22 °C $<$ 800 °C indicate a strength minimum at 400–600 °C and these and higher temperature tests show little or no relative strength decrease from 22 °C levels until $\sim$800 °C and may often show a limited maximum at 600–800 °C (also observed for some fibres, tested in true tension, designated by σ_t in Fig. 4, or flexure).

2.2. BeO

Bentle and Kneifel [41] showed polycrystalline BeO strength averaging $\sim$10% greater at $-$196 than at 22 °C in vacuum, suggesting a possible 15–30% increase for grain sizes $> \sim$40 μm, and a possible $\sim$5–10% decrease at grain sizes of 20–40 μm. They

also showed testing in air or water versus vacuum at 22 °C reduced strengths of BeO ($G \sim 20$ μm) ~8–10%, and 15–20%, respectively. Similarly, Rotsey *et al.* [42] showed a strain rate dependence of BeO ($G \sim \leqslant 3$ μm, $P \sim 4\%$) indicating ~30% strength decrease in water versus air at 22 °C for circumference ground (pressed) rods. Slightly higher strength, but similar relative changes were found in air, but no change in silicone oil. Annealed samples had higher strength, and somewhat higher decreases (~40%) for testing in air, but showed nearly a 10% decrease for tests in silicone oil.

BeO shows a typical Young's modulus decrease with increasing temperatures, e.g. ~15% by 1200 °C [37, 38] (Fig. 5). Tests of (as-grown) single crystals in vacuum at 500 °C and 1000–1800 °C [43] showed slip only at $\geqslant$ 1000 °C, with strengths following the decrease of Young's modulus with temperature fairly closely. Carniglia's earlier σ–$G^{-1/2}$ surveys [25, 26] of BeO showed moderate or no strength decreases at fine grain sizes until > 800 °C, with strength possibly increasing at intermediate temperatures. Though there was less differentiation of strengths versus temperature at larger grain sizes, there was even greater indication of strength, first increasing with increasing temperature, then decreasing. Bentle and Kneifel's [41] data for 500–1300 °C almost always showed a strength maxima at 500–1200 °C which was greater than strengths at 22 °C (Fig. 5). Samples made with 1% MgO ($G \sim 60$–150 μm) showed substantially lower strength maxima. Such maxima were not seen for slightly less (~99.3%) dense samples (e.g. $G \sim 45$ and 60 μm) or greater impurity contents (mainly 5000–7000 p.p.m. F) than those shown in Fig. 5

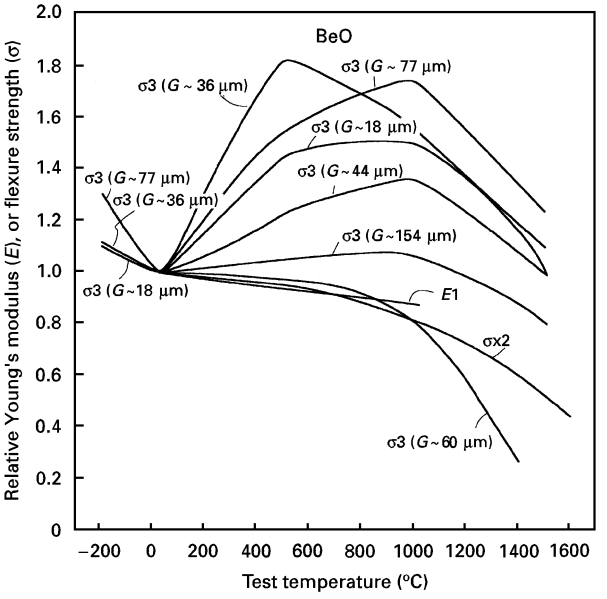

Figure 5 Relative Young's modulus (E and flexure strength (σ) for (as-grown) single crystal and polycrystalline BeO (normalized by taking the value at 22 °C = 1). Curve designations are analogous to those of Fig. 4. Note, Bentle and Millers' (2 [43]) and Bentle and Kniefel's (3 [41]) tests were in vacuum ($G \sim 60$ and 154 μm is with 1% MgO). Data of Fryxell and Chandler (1 [45]) is for both unoriented (open symbols, AOX powder) and oriented (solid symbols, UOX powder), and that E–T trends, especially for single crystals, are a key basis of comparison.

(99.7–99.8% dense); instead strength was approximately constant (e.g. 400–800 °C). Chandler *et al.* [44] tests at 300–1200 °C in air showed moderate (~15–25%) relative strength maxima at 500–1000 °C for 99.9% pure (UOX and HPA) ($P \sim 2$–3%, $G \sim 20$ μm), while a less dense (99.7%) pure (AOX) BeO showed σ–T closely following E–T trends. However, the same AOX BeO with $G \sim 50$ μm ($P \sim 4\%$) showed a strength maxima at 1000 °C, 35% greater than at 22 °C, and UOX BeO with 0.5% MgO rising to a slightly lower maximum. Fryxel and Chandler [45], using the same materials and process, showed all specimens having a relative strength maximum at 500–800 °C with the level of the relative maximum increasing with increasing grain size from 7–10% ($G \sim 20$ μm) through 20% ($G \sim 50$ μm) to 40–43% ($G \sim 90$ μm). There was typically a tendency for lower relative strength maxima with AOX BeO (no additive) than with UOX BeO (+0.5% MgO); the latter also showed preferred orientation increasing with increasing grain size. The absolute strength values were highest (~200 MPa) for $G \sim 20$ μm and intermediate for $G \sim 50$ μm bodies for both AOX and UOX, the latter showing ~50 and ~65% grain orientation for the two grain sizes, respectively. The ~90 μm G bodies had strengths of ~100–130 MPa for AOX and ~130–175 MPa for UOX with ~80% grain orientation. Relative strength maxima at intermediate temperatures were also reported by Stehsel *et al.* [46] for three commercial cold-pressed, and one commercial slip-cast, and fired BeO, and two (both commercial) of four hot-pressed BeO samples tested. While the latter tests and those of Chandler and colleagues were in air, those of Bentle and Kniefel were in vacuum, indicating that these trends (e.g. the maxima) are not due solely, if at all, to environmental (e.g. H_2O) effects. On the other hand, Carniglia *et al.* [47] showed strengths (in vacuum) of dense hot-pressed BeO being ~12% higher at − 200 °C versus in air at 22 °C ($\sigma \sim 270$ MPa), and 45, 51 and 27% higher, respectively, at ~550, 1000 and 1500 °C.

2.3. MgO and CaO

Shockey and Groves [48] showed K_{IC} of MgO crystals increased in H_2O (but not dimethys formamide (DMF)). Both Janowski and Rossi [49] and Rice [50] showed that MgO crystal yield stresses decreased ~20% and strength ~15% (but with greater ductility) in water versus in air at 22 °C. Both showed drying crystal pieces tested in water returned yield and fracture stresses back to their original air-tested levels when retested (dried) in air. Thus, slow crack growth (SCG) has not been observed in MgO single crystals, but yield and fracture stress reductions have been observed indicating enhanced dislocation mobility (as does the increased toughness and ductility). On the other hand, similar CaO crystal tests showed yield and fracture stresses increasing respectively by ~5–25% and 5–35% in water versus air at 22 °C [50]. Testing MgO crystals in liquid N_2 raised yield stresses ~80–130% [50], consistent with Copley and Pask's [51] (compression) and Thompson and Roberts tests

[52], and fracture stresses 10–15% versus in air at 22 °C. Corresponding CaO crystal increases were ~105% and 90%, respectively. However, long-term exposure of CaO crystals to liquid or vapour H_2O results in propagation of cleavage cracks attributed to the wedging action of resultant $Ca(OH)_2$ in preexisting cracks [50].

Polycrystalline MgO tests by Janowski and Rossi [49] and Rice [50] showed strengths lower (e.g. ~15%) in water than in air at 22 °C; i.e. very similar to crystal tests. Both also showed recovery of the strength loss on drying and retesting in air. (Rice's tests covered $G \sim 2$–100 μm, showing no grain size trend.) However, strength in air was only ~10% lower than in liquid N_2; i.e. only ~10% of the difference found for single crystals. On the other hand Rhodes *et al.* [53] reported delayed failure in polycrystalline MgO ($G \sim 25$–45 μm, P (0–0.7%) and $\leqslant$ 0.02–0.6% impurities). While the two finer grain bodies ($G = 26$ & 30 μm) showed delayed failure at ~50% of the inert strength (versus ~80 and 70% for $G = 46$ and 43 μm, respectively) they were also the lowest purity (99.4 and 99.6 versus 99.98 + and 99.92%, respectively). Thus, they concluded that purity was the dominant variable in SCG, which is consistent with most of the impurities being at the grain boundaries [53] with intergranular fracture (in contrast to mostly transgranular fracture in similar grain size bodies tested in air [54]). They also observed a possible fatigue limit (~80%) in the highest purity body which they postulated to be due to the absence of a continuous grain boundary impurity film.

Recrystallized CaO crystal bars at ~1100 and 1300 °C showed little or no strength decrease from 22 °C. However, macroscopic yield frequently preceded brittle, almost exclusively transgranular fracture [50]. Limited polycrystalline MgO studies at moderate temperatures typically showed either an initial limited strength rise to a maxima at 400–700 °C (especially as grain size increased) or a lower rate of decrease before more rapid strength decrease with increasing temperature. These polycrystalline strength trends are also supported by data of Evans *et al.* [55] ($G \sim 25$ and 150 μm, particularly for chemically polished samples). MgO single crystals recrystallized by pressed forging [56] or hot extrusion [57] also showed little or no strength reduction with increasing temperature, some macroscopic yielding by ~1300 °C and extensively at ~1500 °C (but maintaining transparency and subsequent brittle, cleavage fracture). While hot extruded MgO specimens from hot-pressed and annealed billets showed similar strength for the same grain size as from recrystallized crystals at 22 °C, the former showed a greater strength decrease at 1540 °C, and the recrystallized crystals averaged approximately twice the strength as hot extruded, hot-pressed MgO. Similarly, while the latter showed somewhat greater occurrence of grain boundary fracture at 22 °C, it showed much greater frequency and amounts of this at higher temperature than the recrystallized crystals [55, 57]. The above trends (which are consistent with those of Day and Stokes [58], $G \sim 100 \pm 50$ μm, $T \geqslant 1700$ °C) are put in better perspective by plotting properties normalized by their 22 °C values (Fig. 6). This shows: (1) a moderate Young's modulus decrease of 10–15% by 1200 °C; (2) substantially faster yield stress decrease (for ⟨1 0 0⟩ stressing); (3) strength approximately constant or a strength maximum between 400–800 °C; and (4) a trend for less strength decrease, and higher relative maxima at higher temperature as grain size increases.

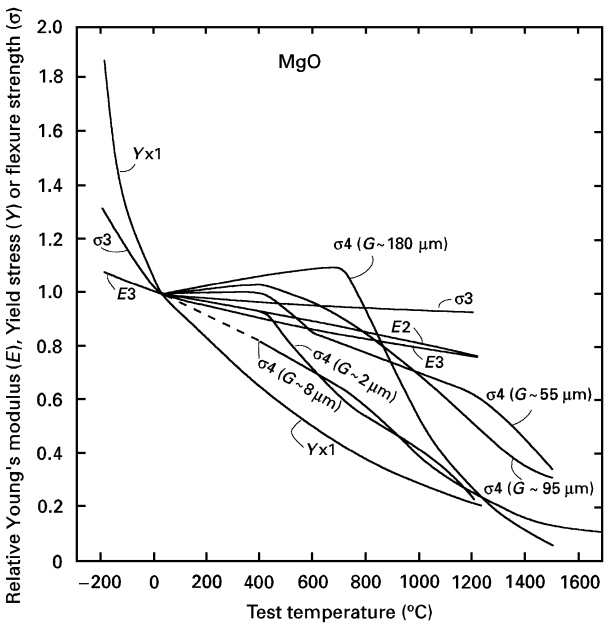

Figure 6 Relative Young's modulus (E), yield stress (⟨1 0 0⟩ single crystal, Y) and flexure strength (σ) of MgO versus test temperature (normalized by taking the property at 22 °C = 1). Note curve designations are analogous to those of Fig. 4, and that E–T trends, especially for single crystals are a key basis of comparison. 1, Copley & Pask [51]; 2, Wachtman & Lam [39]; 3, Neuber & Wimmer [15]; 4, Vasilos *et al.* [59].

2.4. ThO_2 and UO_2

ThO_2 shows positive σ–$G^{-1/2}$ slopes for finer grains at 22 and 1000 °C, but somewhat higher strength at 1000 versus 22 °C across the grain size range studied [50, 61] (Fig. 7). Collectively, UO_2 flexure data [62–66] is consistent with the basic σ–$G^{-1/2}$ model at 22 and 1000 °C, and indicates probable increased strength at 1000 °C (Fig. 8). Diametral compression data [66] at 22 °C also agrees with these trends. Individual data sets more clearly show strength increasing with temperature. Thus, Burdick and Parker [62] showed UO_2 strength increased to a maximum at 700–1100 °C with net increases of 20–35% for $G \sim 20$ μm ($P \sim 15$–22%) and 50–70% at $G >$ ~40 μm ($P \sim 8$–12%). Knudsen *et al.* [63] showed ~20% strength decrease for $G >$ ~45 μm ($P \sim 10$%) and a 5 to 75% increase for $G = 20$–25 μm ($P \sim 8$–24%) between 22 and 1000 °C. Evans and Davidge [63] showed no strength increase with initial temperature increase for their $G = 8$ μm UO_2 till ~500 °C, then a significant rise, peaking at ~800 °C (a ~35% total increase) before decreasing again. Their ~25 μm G body showed a longer, slower strength rise, peaking at ~1100 °C with a similar net

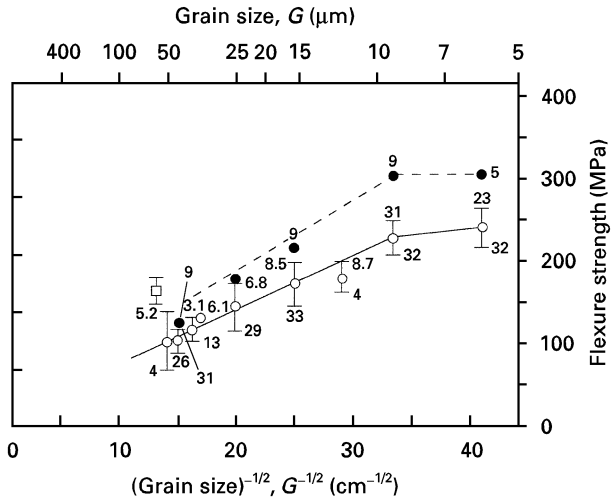

Figure 7 ThO_2 σ versus $G^{-1/2}$ at 22 and 1000 °C. Data of Knudsen [59] corrected for variable P (superscripts are $\%P$) using $b = 4.2$, and 6.6 at 22 (○) and 1000 °C (●), respectively, per his analysis. Numbers with high temperature data points and below the error bars for tests at 22 °C are the number of values averaged. Note the consistency of resultant corrected data despite quite variable P levels for different G bodies. The one data point from Curtis and Johnson (□ [60]) is also shown.

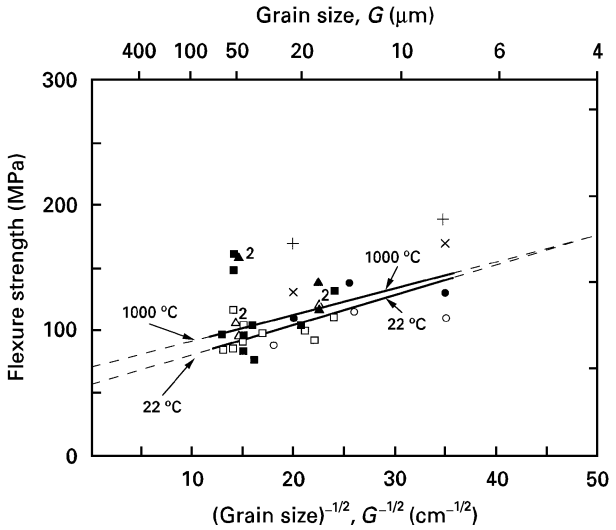

Figure 8 UO_2 σ versus $G^{-1/2}$ at 22° (open symbols) and 1000 °C (filled symbols). Data of Burdick and Parker (△, ▲ [61]), Knudsen *et al.* (□, ■ [62]), Evans and Davidge (×, + [63]) and Canon *et al.* (○, ● [65]) are for flexure at both temperatures. That of Kennedy and Bandyopandhyay [66] is only at 22 °C and from diametral compression. Note data plotted as-measured with $P \sim 2\%$ for Canon *et al.* and ~3% for Evans and Davidge, while Knudsen *et al.*'s data was corrected for P(= 5–24%, mostly 5–10%) and Burdick and Parker ($P = \sim 8$–12%) using $b = 3$ (a 2 next to some data points indicates two identical points). Data of Kennedy and Bandyopandhyay plotted as-measured for $P = 3$–9% (shown next to data points). Note there is no trend for strength to decrease from 22 to 1000 °C, and in fact strength appears to be greater at 1000 than 22 °C.

increase, before decreasing. Beal *et al.* [64] showed a similar σ–T increase and maximum strength ($G \sim 25$ μm, $P \sim 3\%$). Canon *et al.* [65] showed strength increased slowly to a maximum (about 20% higher than at 22 °C) at ~1400 °C, then dropped sharply, for bodies with $G = \sim 8$, ~15 and ~31 μm.

2.5. ZrO_2

While ZrO_2 single crystals (11.1 mol %, ~18.5 wt % Y_2O_3) show a typical Young's modulus decrease (e.g. ~1–2%/100 °C) with increasing temperature to the limit of testing (700 °C), polycrystalline behaviour is more complex [68]. Polycrystalline ZrO_2 (CaO or MgO) stabilized showed somewhat greater Young's modulus decreases to ~400 °C, then transitions to an approximate extrapolation of the above single crystal data [5, 68]. Wachtman and Corwin [69] showed an internal friction peak in ZrO_2, generally in the 300–400 °C range, but decreasing somewhat in magnitude and in the temperature of the maximum as the CaO content increased from 2 to 20%. Shimada *et al.* [70] showed an initial somewhat greater Young's modulus decrease to ~400 °C, then (within the 650 °C limits of testing) a similar transition as above for dense ($P \sim O$) sintered ZrO_2(+3 m/o, ~5.5 w/o Y_2O_3), as have Adams *et al.* [71] for sintered ($P \sim 2$–7%, $G =$ 15–50 μm) and hot-pressed ($P \sim 0.5$–2%, $G \sim 1$–3 μm) ZrO_2(+6.5 m/o, ~11 w/o, Y_2O_3). Adams *et al.* [71] also showed their ZrO_2–Y_2O_3 (and a commercial ZrO_2–Y_2O_3) body (with ~1 w/o SiO_2) had much greater Young's modulus decrease from ~100 to ~400 °C than three commercial ZrO_2–MgO bodies tested. Rapid initial E–T decreases have also been more recently reported for: (1) ZrO_2 +33 m/o Tb_4O_7 between 200 and 500 °C (but not with 33 m/o Pr_6O_{11}) [71]; (2) 3 m/o Y_2O_3 between ~22 and 300 °C [73]; and (3) 2 m/o Y_2O_3, +8 m/o Y_2O_3, and 12 m/o CeO_2 (with respectively similar, greater and smaller decreases, the latter when the CeO_2 was partly reduced, but no effect when it is fully oxidized) [74]. In the latter two cases, as well as that of Shimada *et al.*, the anomalous Young's modulus decreases were associated with maxima or high levels of internal friction. Nishiyama *et al.* [75] also recently reported an internal friction peak at ~150 °C in ZrO_2–2.8 m/o Y_2O_3. These ZrO_2 changes are corroborated by similar effects of Dole and colleagues [18, 76] in HfO_2, i.e. an internal friction peak in unstabilized (monoclinic) HfO_2 at ~400 °C, and drops in both Young's and shear moduli and an internal friction peak in HfO_2–20 m/o Er_2O_3.

While fully stabilized ZrO_2 crystals (22 w/o Y_2O_3) show essentially no strength changes till $T \sim 1500$ °C [76], polycrystalline strengths show similar, but greater deviations from E–T trends (Fig. 9). Thus, the lack of significant single crystal strength changes between −196 and 22 °C indicates limited, or no, single crystal SCG. Partially stabilized (6 w/o Y_2O_3) crystals (which start from approximately four fold higher strength than fully stabilized crystals) show an initial strength decrease much greater than that of Young's modulus until ~500 °C, then levelling off (at about twice the strength of fully stabilized crystals) until ~1500 °C. Adams *et al.*'s tests of sintered and hot-pressed ZrO_2 (+ ~11 w/o Y_2O_3) [71], though scattered, showed an average initial trend similar to the PSZ (6% Y_2O_3), crystals, but continued to have much greater strength as Young's modulus decreases, to a modest minimum at ~700 °C. Drachinsku *et al.* [78] showed a slightly greater strength decrease to the

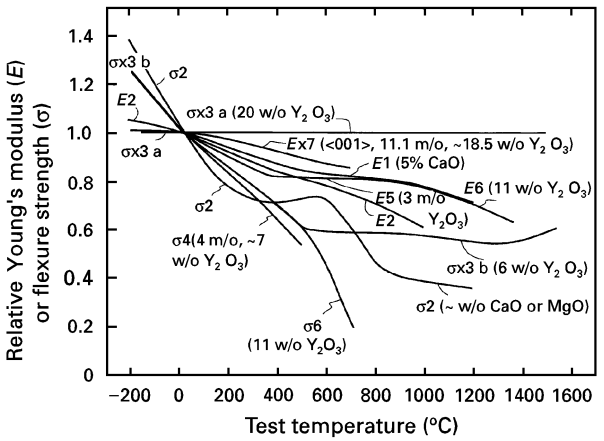

Figure 9 Relative Young's modulus (E) and flexure strength (σ), of single- and polycrystalline ZrO_2 versus test temperature (normalized by taking the property at 22 °C = 1). Note the stabilizer in Neuber and Wimmers' ZrO_2 is not specified but is believed to be either CaO or MgO (~5 wt %, $P \sim 13$ %, $G \sim 25$ μm). Note curve designations are analogous to those of Fig. 4 (along with designation of some compositions), and that E–T trends, especially for single crystals are a key basis of comparison. 1, Wachtman & Lam [39]; 2, Neuber & Wimmer [15]; 3, Ingel *et al.* [77]; 4, Drachinskii *et al.* [78]; 5, Shimada *et al.* [70]; 6, Adams *et al.* [71]; 7, Kandil *et al.* [68].

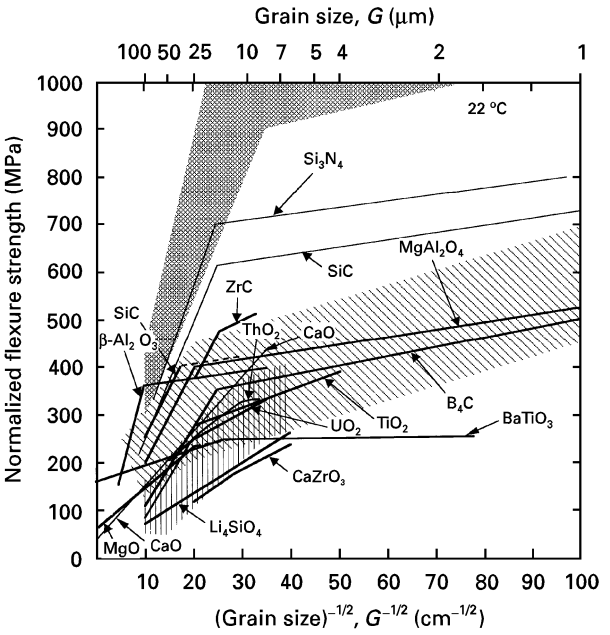

Figure 10 σ–$G^{-1/2}$ data for various ceramics at 22 °C normalized to the same Young's modulus as for Al_2O_3 (~400 GPa, i.e. the σ plotted is that of the material $400/E_m$, where E_m = Young's modulus of the material (from Table I). (■) ZrO_2; (▥) BeO; (▨) Al_2O_3.

limits of their tests (500 °C, Fig. 9) in ZrO_2 + 4 m/o (~7 w/o) Y_2O_3 sintered then annealed substantially. However, specimens with limited annealing after sintering dropped to a strength minimum of ~80% their 22 °C values at 100–200 °C, then rose to a strength maxima at 300–400 °C that could be similar or greater (e.g. ~35%) than strengths at 22 °C. Higher temperature tests of some of these lesser annealed samples showed first a strength minimum at ~700 °C (like Adams *et al.*), but strength values ranged from 50% relative to 22 °C down to ~30% relative to their strength maxima at ~300 °C (i.e. in either case less relative decreases than for Adams *et al.*), then a strength maximum at ~1000 °C. Such greater strength deviations and complexities are apparently not limited to ZrO_2–Y_2O_3 bodies, as shown by Neuber and Wimmer [5] reporting greater strength than Young's modulus decrease with increasing temperature, and probable inflections at ~300 and 800 °C (Fig. 10) in ZrO_2 (with ~5 w/o CaO or MgO).

Fracture mode changes accompany the above ZrO_2 strength decreases with increased temperature (Fig. 9), e.g. Adams *et al.* [71] saw mostly transgranular fracture at 22 °C, mixed trans- and intergranular fracture at 1000 °C, and 100% intergranular fracture by 1500 °C in their ZrO_2 (~11 w/o Y_2O_3) bodies, similar to PSZ (2.4 w/o MgO) [76]. Drachinskii *et al.* [78] observed transgranular fracture varying from 40 to 90% for specimens of various annealing in tests at 100 °C, with the least transgranular fracture being for the lowest strength (180 MPa), but an intermediate percentage (70%) for the highest strength (410 MPa), versus 90% at 370 MPa. Rice [79] has observed fracture initiation from grain boundaries surrounded entirely by 100% transgranular fracture not only in MgO, CaO and $MgAl_2O_4$, but also ZrO_2 (12.4 w/o MgO) and ZrO_2 (+ 11 w/o Y_2O_3 – from the same processing as specimens used by Adams *et al.*). The substantial intergranular fracture at higher temperatures correlates with substantial grain boundary sliding creep, and even superplasticity found at ⩾ 1000 °C in fine grain TZP [80].

2.6. $MgAl_2O_4$

Stewart and Bradt [81] showed (indentation fracture) K_{IC} of $MgAl_2O_4$ crystals decreasing (~20%) to a minimum at ~900 °C for {1 0 0} fracture (and less for other orientations). They [82] also showed K_{IC} of hot pressed $MgAl_2O_4$ decreasing slowly with increasing temperature (e.g. ~10% by ~900 °C) for G = 5, 12 and 25 μm (but possibly less for G = 40 μm). At ~900 °C and beyond, K_{IC} decreased much more rapidly. Ghosh *et al.* [83] showed the work of fracture of dense $MgAl_2O_3$ ($G \sim 35$ μm) constant to ~800 °C, then increasing. On the other hand strength was essentially the same at 22 and 200 °C, dropped by ~25% to a minimum at ~600 °C or a plateau at ~400–800 °C, then decreased slowly at higher temperature, i.e. similar to the temperature dependence of Young's modulus [82].

2.7. Borides, carbides and nitrides

Limited tests of ZrB_2 at 1000 °C showed no strength change from 22 °C [84] or a maxima at ~300 °C (~600 °C for HfB_2, both in inert atmosphere) [85]. Inert atmosphere tests of TiB_2 showed strengths progressively higher at ~1000 and 1300 than 22 °C [86]. Similar tests of SiC showed strength and K_{IC} maxima at ~1400 °C [87], and considerable investigation of dense sintered and hot-pressed SiC for engine and other applications commonly showed strength at 1000 °C similar to that at 22 °C, or somewhat

(e.g. ~20%) higher (typically for $G \sim 2$–10 μm) [88]. Several investigations [89–92] showed strengths of B_4C decreasing very little until ~800 °C (and limited decrease above 800 °C) [89], which is consistent with K_{IC} [90–92], trends. Miracle and Lipsitt [93] showed limited (e.g. 10–20%) strength increases or decreases, or possibly no strength changes, in TiC from 22–600 °C, and in some cases to 1000–1200 °C depending on C/Ti ratios of 0.66, 0.75, 0.83 and 0.93 (G, respectively, 22, 21, 20 and 14 μm). Substantial strength decreases occur at higher temperatures, with the earliest and greatest strength decrease for the C/Ti = 0.66, $G \sim 22$ μm body. Thus, the strength change with increasing temperature generally did not follow the ~5% decrease of Young's modulus in this temperature range [93]. More extensive testing of dense sintered or hot-pressed Si_3N_4, as well as less dense RSSN shows some bodies had lower strengths by 800–1000 °C versus 22 °C, many had no decrease, and several increased (again by up to ~20%) [88]. This again shows strength not following the E–T trend (e.g. ⩽ 5% decrease by 1000 °C [94]). Although such increases are most common for RSSN, they are not restricted to it (increases in strength can result from surface oxidation removing flaws in such non-oxides, especially RSSN).

3. Discussion

3.1. Overall strength–grain size behaviour

This and other papers [1–4, 8] clearly show σ–$G^{-1/2}$ behaviour follows a two-branched curve at ~22 °C. The finer grain branch(es) show limited, while the larger grain branches show substantial grain size dependence of strength. For microplastic controlled strength, the larger grain branch approximately extrapolates to the single crystal strength reflecting the easiest mode of microplasticity activation [54, 55, 57]. For brittle fracture, the larger grain branch commonly extends below, often substantially, the lowest single crystal strength (as a function of orientation) for comparable surface finish. Where microplasticity occurs, it competes with flaw failure, with the balance between the two failure mechanisms often being shifted by specimen quality (i.e. processing defects), surface finish, temperature, and possibly test environment [57].

For brittle fracture $\sigma \propto \sqrt{E\gamma}$, but $\gamma \propto E$ [95], and hence $\sigma \propto E$, as also shown experimentally [96], making it useful to normalize temperature effects on Young's modulus and strength. Normalizing strength data at 22 °C (to $E = 400$ GPa for Al_2O_3, using E values in Table I) brings most materials' σ–$G^{-1/2}$ behaviour closer (Fig. 10). This results in no distinction whatsoever between cubic and non-cubic materials, indicating that such structural differentiation does not correspond to any basic σ–$G^{-1/2}$ trends. Further, there is no clear difference for materials where microplasticity can determine strength; e.g. CaO [1, 50, 56], MgO [1, 54, 57] and $BaTiO_3$ [97]. The one possible differentiation that may be indicated in Fig. 10 is that between oxides and some non-oxides, i.e. the latter (e.g. reflecting more covalent bonding) tend to be in the upper half of the range (except for the special case of transformation toughened ZrO_2). Whether this reflects intrinsic differences or simply more successful development cannot yet be determined.

While less σ–$G^{-1/2}$ data exists at elevated temperature, sufficient does exist (mainly at 1000–1300 °C) to show basic similarities with behaviour at 22 °C, i.e. the common occurrence of two branched σ–$G^{-1/2}$ curves, often higher strength levels for non-oxides, and limited differentiation of microplastic and flaw failure (Figs 11 and 12). A possible difference is that materials such as ThO_2 and UO_2, which may become in part controlled by microplasticity, may have higher relative strengths

TABLE I Young's moduli used to normalize ceramic σ–G

Material	Young's modulus (GPa)
Al_2O_3	400
TiO_2	285
BeO	395
MgO	355
Mg–Al_2O_4	294
ThO_2	250
UO_2	230
ZrC	400
SiC (β)	400
CaO	200
ZrO_2	230
β-Al_2O_3	~ 200
Li_4SiO_4	138
$CaZrO_3$	180
$BaTiO_3$	190

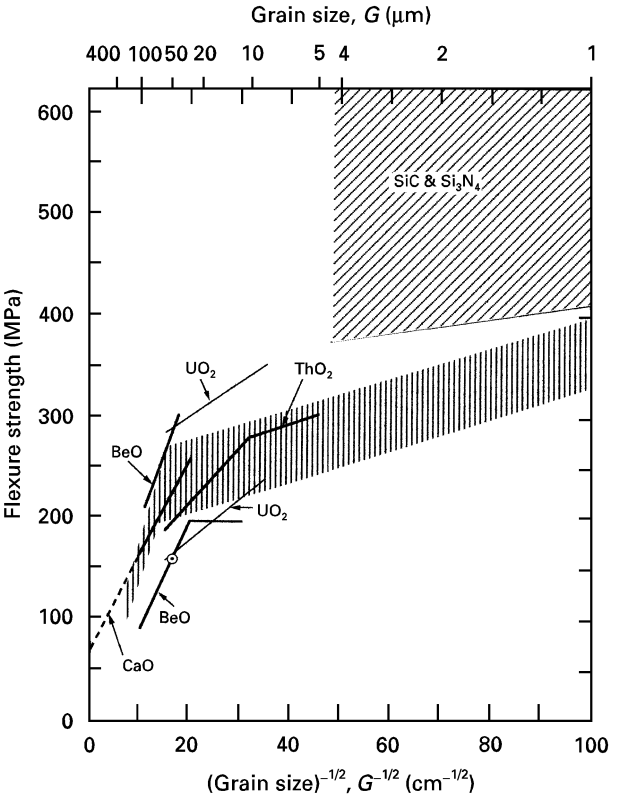

Figure 11 σ–$G^{-1/2}$ data for various ceramics at ~1000 °C normalized to the same Young's modulus as Al_2O_3 (as in Fig. 10, per Table I). ((▥)) Spriggs & Vasilos [32]; (⊙) Davidge & Tappin [6] ($P \sim 3$–5%).

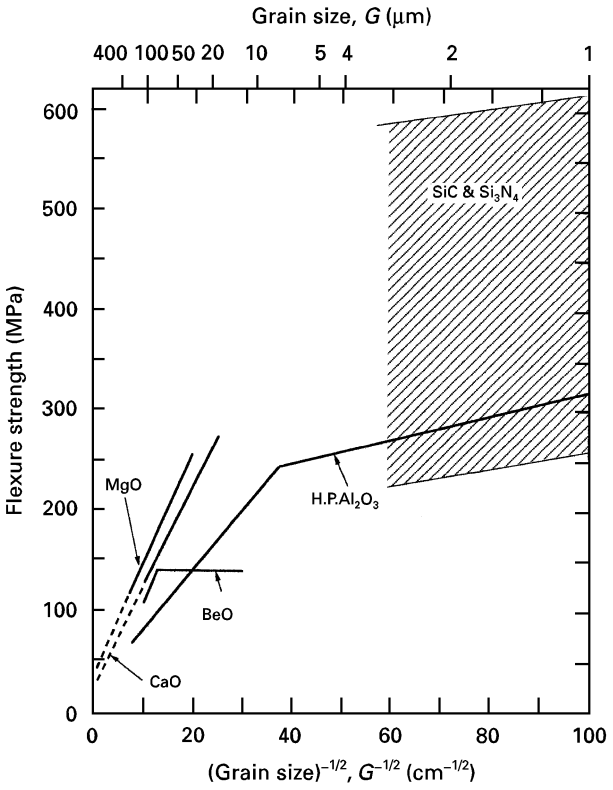

Figure 12 σ–$G^{1/2}$ data for various ceramics at $\sim$1200 °C normalized to the same Young's modulus as Al_2O_3 (as in Figs 10 and 11, per Table I).

than at 22 °C, but much more study of dense, quality bodies as a function of grain size and temperature is needed.

This survey shows that substantial strength changes can occur in the (often neglected) regime of less than 1000 °C. Thus, significant changes of the relative single- and poly-crystal strengths may occur, and there may also be variation of these changes with grain size. Parameters affecting such variations include not only environment (i.e. mainly H_2O here) and temperature, but also surface finish (especially machining effects). Further, possible effects of material parameters (e.g., TEA and elastic anisotropy, EA) vary with temperature, microstructure and possibly environment, as do effects of surface finish (environmental effects are also a function of temperature). However, effects of environment and surface finish can be at least partly separated out, though studies have not often done this. First, effects of the test medium (i.e. of H_2O environmental effects) are addressed, then the effects of temperature and its interactive effects are addressed in the next section.

3.2. Effects of test medium

Except in special cases (discussed later) environmental interactions with slip or twinning, can be neglected, as can effects of temperature via Young's modulus (e.g. $\sim$1–2%/100 °C). Environmentally induced slow crack growth (SCG), while particularly pertinent to the large grain regime, since crack growth plays an intrinsic role in brittle fracture there [1, 98–102], also affects the finer grain regime [1, 7], either or both effects impacting the intersection of the finer and larger grain branches. The occurrence of SCG in single crystals indicates that transgranular SCG can occur in polycrystalline materials and thus may not impact the single–poly-crystal strength balance. SCG occurs in sapphire, at rates generally similar to those of polycrystalline Al_2O_3 [103]. (This implies similar SCG on key sapphire fracture planes, although this has not been directly established). However, SCG in Al_2O_3 tends toward more intragranular fracture, especially at finer grain (along with possibly greater SCG at finer grain size), in contrast to more transgranular fracture commonly observed in fast fracture. SCG also occurs in polycrystalline BeO [41], where the specifics of the SCG fracture mode are poorly documented (the overall fracture mode for tests in air at 22 °C is predominantly transgranular) [41]. While SCG does not occur in some single crystals such as MgO and apparently ZrO_2, it can occur intergranularly in MgO, as shown by Rhodes *et al.* [53]. More SCG in finer versus grain MgO ($\sim$25 μm versus $\sim$45 μm) is uncertain because of impurity differences [53], but may imply a grain size effect in view of there typically being more grain boundary phase as grain size increases. Whether there are intrinsic differences in SCG rates between materials exhibiting only intergranular versus at least some transgranular SCG is unknown. In contrast to the above oxides, fast fracture in a Mn–Zn ferrite [104] was predominantly by intergranular fracture, while SCG occurred mostly by transgranular failure, especially with $G \sim 45$ μm and somewhat less in with $G \sim 35$ μm with more grain boundary (e.g. Ca) phase, again suggesting possibly greater effects at finer grain size. Li ferrites show SCG which has also been reported to be sensitive to losses of Li on firing [105] which may imply gradients of stoichiometry between grain boundaries and the rest of the grain, which could be a factor in changing fracture modes and in possible grain size effects.

Regarding non-oxides, SCG has been shown in some halide single crystals e.g. AgCl and CaF_2 (the latter also showing probable effects of slip limiting the extent of SCG, e.g. via easier arrest of cracks [103]). SCG in polycrystalline MgF_2 and ZnSe being 100% intergranular (whereas fast fracture is essentially 100% transgranular) indicates grain boundary control of SCG in these materials [103]. McKinney *et al.* [106] reported essentially no SCG with large scale cracks, e.g. double cantilever beam (DCB) or double torsion tests, in various Si_3N_4 materials and no small scale SCG (i.e. no delayed failure in pure Si_3N_4, made by either chemical vapour deposition (CVD) or reaction sintering), but clear delayed failure in Si_3N_4 made with oxide additives (with the extent of SCG generally increasing with the amount of oxide additive) via 100% intergranular fracture. They attributed this large versus small crack behaviour to oxide distribution along grain boundaries, i.e. that of the many flaws available on the surface for SCG, at least one could always be found that had sufficient contiguity of grain boundary oxides for sufficient SCG to lower strength. On the other hand, large cracks, as used in a DCB test,

covered too broad a range of grain boundaries, many of which may not have sufficient oxide content or contiguity to allow continuous SCG. Recently SCG has been reported (via essentially 100% intergranular fracture) in AlN [107, 108] on a similar or lower level than in Al_2O_3 [103]. While there appears to be intrinsic SCG in carbon materials [102], SCG does not appear to occur in carbides, e.g. B_4C, SiC, TiC and ZrC (or borides, e.g. TiB_2 and ZrB_2) unless sufficient grain boundary phase (e.g. oxide) is present to provide the material and path for SCG [109]. Thus, SiC made with oxide additives shows SCG, but not SiC made by CVD (i.e. without additives), i.e. paralleling the Si_3N_4 results. This is corroborated by such materials showing no SCG exhibiting predominant to exclusive transgranular fracture, while those showing SCG have substantial intergranular fracture [109].

3.3. Effects of test temperature on Al_2O_3 and BeO

The temperature dependence of strength and related properties (E and K_{IC}) is important in elucidating the effects of SCG and broader understanding of failure mechanisms, but can be complex. Thus, it significantly effects slip or twinning and microstructural stresses, e.g. due to TEA as well as local redistribution of applied stresses due to EA, and changing surface conditions, e.g. relaxing compressive stresses from finishing. The complexity, as well as the possible insight that can be gained is better seen from the relative temperature dependence of Al_2O_3, BeO, MgO and ZrO_2 (for which there is reasonable data, Figs 4–6 and 9). Thus for $T < 600$–$800\,^{\circ}C$, Al_2O_3 and BeO, both non-cubic materials with similar, significant TEA show opposite σ–T trends, i.e. BeO strength increases with temperature while Al_2O_3 strength decreases, especially for crystals with no TEA.

The initial, substantial Al_2O_3 strength decrease, previously speculated to be due to increasing crack tip microplasticity, i.e. slip or twinning, is countered by crack tip dislocations not being found by Wiederhorn *et al.* [21]. On the other hand, a number of observations suggest a possible explanation for the sapphire $\sigma - T$ minimum based on twinning as follows. Heuer [110] reported twins introduced in sapphire by either surface scratching or fracture (e.g. rhombohedral twins at least as low as $-196\,^{\circ}C$), possible cracks following twins, possible crack nucleation by twin–twin and twin–grain boundary intersections, and twins being thicker and larger above $600\,^{\circ}C$. Becher [111] showed both rhombohedral and basal twins introduced by surface abrasion and frequent association with resultant surface cracks. He subsequently indicated probable cracks along basal twin–matrix interfaces [112]. Scott and Orr [113] showed the resolved shear stress for rhombohedral twinning dropping from $\sim$225 MPa at $\sim 320\,^{\circ}C$ to ~ 5 MPa by $\sim 600\,^{\circ}C$, and remaining constant thereafter to $\geqslant 1500\,^{\circ}C$. Though Scott and Orr's tests were in compression (requiring shortening of the specimen), thus not necessarily reflecting tensile behaviour (requiring elongation), their changes closely mirror the strength changes of sapphire, suggesting cause and effect i.e. similar twinning in tension. The alloying effects reported by Sayir [24] support this. The K_{IC} results of Iwasa and Bradt [23] might appear to question this. However, being obtained by the (Knoop) indentation-fracture tests, they are thus essentially a strength test and indents are common sources of twins [111, 114] (Twin–matrix interfaces could have lower K_{IC}, and be preferred sites for SCG, e.g. be consistent with the marked strength drops in, at least machined, sapphire due to both increasing temperature and environment effects. Annealed surfaces may also have twin–flaw combinations, e.g. from previous machining, or handling but reduced in extent or severity, e.g. as possibly indicated by Charles [15] data for annealed sapphire). There is also evidence that twinning is associated with tensile failure in $BaTiO_3$ single- and poly-crystals [115].

Twinning could be consistent with Al_2O_3 σ-G effects via grain size limiting twin size at moderate and large grain size, but not in the finer grain branch where too many grains are encompassed by the flaw size (C) for individual grain–twin interactions to be significant. Thus, the substantial scatter of Kirchner and Gruver's hot-pressed Al_2O_3 strength minima and maxima data [27, 28] with $C \sim 20\,\mu m$, and $G \sim 2$ $-5\,\mu m$) may reflect effects of known grain heterogeneity. Also, Mizuta *et al.*'s [29] lack of a strength minima is consistent with their apparently uniform, fine grain size. Al_2O_3 fibres, while not being tested as low as 400–500 °C, would be constant with no minimum due to the fine grain size (but a maximum at 800–1100 °C). Neuber and Wimmer's strength minima (and maxima) at intermediate grain size is consistent with such a twinning mechanism, as are Charles' (His larger grain, lamp envelope Al_2O_3 showing less of a strength minima and at higher temperature suggest that environmental factors may also play a role in these σ–T minima and maxima, as speculated above.) Only a suggestion of a strength minimum in tests of Jackman and Roberts [19] ($G \sim 50\,\mu m$) may be due to the probable larger pore size of the residual ($\sim$5%) porosity frequently being a key factor in failure. However, the role of TEA stresses cannot be neglected since, for example, large (e.g. isolated) grains are often preferred sources of failure in Al_2O_3 (and other non-cubic materials) [1].

The subsequent significant strength up-turn and resultant relative σ–T maximum of much of the Al_2O_3 data (e.g at $\sim$800–1000 °C) could reflect crack tip blunting due to plasticity in single crystals since slip and twinning are clearly observed to occur to an increasing extent in this e.g. 600–1000 °C, range, including at crack tips [21]. However, this is unlikely to be significant in polycrystalline Al_2O_3, especially as flaw size (C) becomes progressively greater than the grain size ($C > G$), since crack tip stress relief encompassing a number of grains is much less likely in view of the limited number of slip and twin systems. Instead of (or in addition) to such microplastic effects, reduction of TEA stresses [116] must be considered. The strength maximum occurs at, or close to, the temperature range at which such stresses are believed to disappear, e.g. based on spontaneous microcracking

from such stresses [116]. Evidence has been presented that such stresses increasingly directly contribute to failure at 22 °C as the flaw size approaches the grain size [115, 117, 118] i.e. pertinent to much of the larger grain branch, with decreasing effects as grain size decreases along the fine grain branch. On the other hand, K_{IC} at 22 °C (measured with large cracks) commonly shows a maximum at intermediate grain size attributed to microcracking from TEA stresses [119]. The latter effects are believed to generally not be pertinent since flaws controlling strength are commonly not on a sufficient scale in the pertinent grain size range. However, the specifics of both of these mechanisms, their possible interactions, and their actual temperature dependence is, at best, very limited.

Reductions in TEA stresses with increasing temperature is a possible mechanism for the BeO σ–T maximum, as originally suggested by Bentle and Kniefel [41] and Clarke [120]. Again the temperature range of the maximum (500–1000 °C) approaches that estimated for the disappearance of TEA stresses based on microcracking from such stresses, [116]. Also, other factors, such as greater grain boundary stress relief due to higher stress in testing than for spontaneous cracking (i.e. with no external stressing), could reduce the temperature for maximum strength. Particularly supportive of such a stress relief mechanism is the absence of any apparent single crystal complications as for Al_2O_3. Again, stress-relief mechanism should be dependent on C not being much greater than G since the effect of such stresses tends to zero when averaged over many grains [1–4, 117]. The indicated grain size dependence of the σ–T maxima (e.g. at $G \sim 40 - 100\,\mu m$) supports this postulate. However, note that reduction of TEA stresses as an explanation of the σ–T maxima, also means that SCG effects may be underestimated by tests in liquid N_2, since this increases TEA stresses, which would thus limit strength increases due to reduced SCG at $T > 22$ °C.

Clearly, grain boundary phases can play an important, but variable, role in the σ–T behaviour, especially beyond ~600 °C. Thus SiO_2-based grain boundary phases in Al_2O_3 can not only relieve TEA stresses, but also lead to grain boundary sliding and attendant strain rate dependent maxima [12, 30] (Fig. 3), as can grain boundary phases in other oxides and non-oxides (e.g. Si_3N_4). This is also shown by less pronounced maxima, or only an approximate strength plateau in BeO with additives or impurities [41]. Such differences probably reflect interrelated effects of the boundary phase and its degree of wetting, which can also be a function of processing, e.g. less SiO_2 wetting of Al_2O_3 under reducing conditions [120], as indicated by differences between commercial (air) sintered ~95% Al_2O_3 [30] and Al_2O_3 hot pressed with 3% SiO_2 [9] (Fig. 3).

3.4. Effects of temperature and elastic anisotropy on cubic and other materials

Turning to cubic materials where there is no TEA, slip can play a role in the strength and fracture of some materials, e.g. CaO and MgO, at room and moderate temperatures, being in competition with flaw failure, with higher temperature increasing the balance for slip [57]. Limited differences between slip and flaw controlled failure in high quality MgO at low and moderate temperature do not appear to explain the marked σ–T differences between such MgO and other materials in this range. At $\geqslant 1000$ °C MgO and especially CaO begin to show some macroscopic deformation and related effects (e.g. strain rate sensitivity), as may ThO_2, UO_2 and cubic (i.e. fully stabilized, single phase) ZrO_2 [76]. However, for $T < \sim 1000$ °C, microplasticity does not appear to be a major differentiator of behaviour, except for special materials (e.g. partially stabilized zirconias and some alkali halides). Its most general effect is via surface work hardening and resultant surface stresses which occur over a broad range of cubic and non-cubic materials [11].

Clearly, a major difference between partially stabilized ZrO_2 (PSZ) and MgO (and other ceramics) is transformation toughening below ~1000 °C. This certainly is a major factor in PSZ strength decrease to at least ~600 °C (Fig. 9) and may be a limited factor in E–T changes (due to possible differing E–T behaviour of the different ZrO_2 phases). However, this does not explain why fully or partially stabilized ZrO_2, especially with Y_2O_3, shows similar, often more extreme (in terms of amount, temperature extent or both) Young's modulus and strength variations with temperature (Fig. 9). The anomalous Young's modulus decrease of ZrO_2 (especially with Y_2O_3 or reduced CeO_2 additions) has been related to oxygen defects, e.g. forming anisotropic complexes as indicated by correlation of internal friction and other loss measurements via conductivity and dielectric tests [73, 74]. Variations with the stabilizer type, amount and reduction (of CeO_2 [73]) lends strong support to this mechanism. Both the oxygen defect nature of the effect and changes with degree of reduction of CeO_2 clearly show the probable importance of ZrO_2 reduction. While this has often been neglected or associated with darkening attributed to other effects [122], this is likely to be important due to reducing conditions in hot pressing or HIPing samples, and especially high-temperature heat treatment of PSZ [123] (usually achieved via induction heating of carbon). Such defect effects have been indicated in ThO_2 [124], and are likely to occur in other materials, e.g. CeO_2 and $MgAl_2O_4$ (i.e. the latter E–T [35] and σ–T jog at 500–700 °C, as noted earlier). While Young's modulus decreases would contribute to σ decreases, the latter are much larger, indicating an enhancement of above oxygen defect mechanism or addition of one or more other mechanisms.

Impurities, especially at grain boundaries, are a possible factor in the ZrO_2 σ–T decreases, especially in view of observed increased intergranular fracture initiation with temperature versus mostly transgranular at lower temperature. However, it is not clear why ZrO_2 should be so much more sensitive to impurities nor why they would be a factor at such low temperatures (e.g. 200–400 °C). While, as noted earlier, SCG was not observed in Y_2O_3 fully stabilized crystals,

polycrystalline SCG via grain boundaries may be a possibility, but extensive transgranular fracture at and near 22 °C argues against this. Destabilization of partially stabilized ZrO_2 by H_2O has also been observed, but only for a modest range of temperature, grain size, and Y_2O_3 content, not explaining similar effects for CaO, MgO or Tb_4O_7 stabilization or full stabilization with Y_2O_3. Further, this effect appears to be a corrosion phenomena [125–129], not SCG; i.e. degradation over the exposed area, not just at tips of sufficiently stressed cracks. Attributing moderate temperature decreases in ZrO_2 mechanical properties to attack of H_2O (or other species such as HCl [125, 126]) also appears inconsistent with some similar strength trends for both $ZrO_2 + Y_2O_3$ single- and poly-crystals (in view of probable association of this H_2O effect with grain boundaries, hence not pertinent to single crystals). This would also possibly imply some opposite effects of H_2O and boundary impurities since the latter may often interfere with the reaction with H_2O. H_2O effects also appear to be inconsistent with many of the property changes continuing well beyond the temperature range of this destabilizing mechanism. Thus, while H_2O effects may contribute to the E–T and, especially, σ–T changes they cannot be the fundamental cause of them.

Another possibility for the σ–T decrease and other effects is elastic anisotropy (EA) which could complement either of the above possibilities, and may be a factor in a number of other materials. EA is particularly pertinent to cubic materials since they lack TEA (which is likely to dominate in non-cubic materials) and often have greater EA than non-cubic materials [130–132]. For cubic materials a common measure of EA is A^*

$$A^* = \frac{3(A-1)^2}{3(A-1)^2 + 25A}\left(A = \frac{2C_{44}}{C_{11} - C_{12}}\right) \quad (1)$$

Amongst cubic ceramics, ZrO_2 [131, 132] UO_2, $MgAl_2O_4$, β-SiC, ZnS and ZnSe have high EA (e.g. 5–10%, which means that the ratios of maximum to minimum Young's moduli are 1.5–2). This raises the question: is higher EA related to intergranular SCG, e.g., in large G ZnSe bodies, and possibly in ZnS [131]? Correlations of grain boundary cracking around hardness indents has been indicated with EA of cubic materials and combined EA and TEA effects in non-cubic materials [133]. While EA may decrease or not change much with increasing temperature for some materials, it shows considerable increase with temperature for several materials recently reviewed [131], e.g. CaO, MgO and ZrO_2. The latter shows EA increases significantly in the temperature range where Young's modulus and strength show marked decreases (Figs 9 and 13) and shows substantial composition dependence, implying even higher EA for partially stabilized materials (e.g. those of Drachinskii *et al.*) [77].

The similarity of TEA and EA providing local (grain boundary) stress concentrations (the latter, only with an external stress applied to the body) might suggest EA as an analogous possibility for some (e.g.

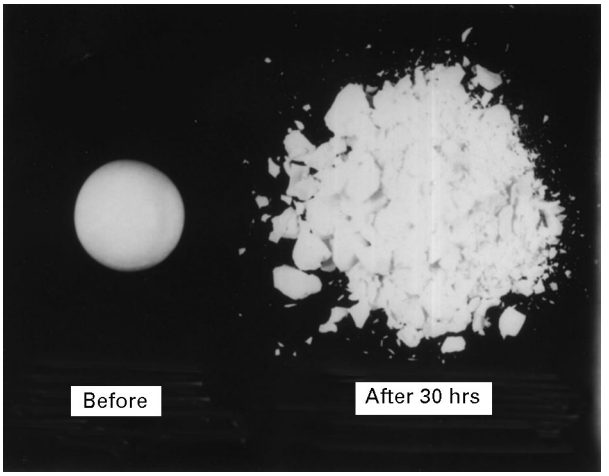

Figure 13 Example of the degradation of (commercial) $ZrO_2 + Y_2O_3$ in 690 kPa steam at 200 °C in 30 hours. Photo courtesy of Dr T. Quadir [128].

MgO) σ–T maxima at intermediate temperature, i.e. as for TEA as a possible cause of such maxima in Al_2O_3 and BeO. However, the common continued rise of EA with temperature noted above would appear to rule this out [132] (TEA stresses decrease with increasing temperature). On the other hand, increasing deformation with temperature combined with EA–T changes might be a possible mechanism. Such EA contribution would probably increase with grain size, analogous to the grain size dependence of spontaneous cracking from TEA [108].

The marked EA of ZrO_2 may correlate with the occurrence of grain boundary fracture origins in larger grain bodies, fully and partially stabilized ZrO_2 [132]. The temperature rise of ZrO_2 EA may also contribute significantly to its higher temperature grain boundary sliding [71]. Further, since EA increasing with temperature is very broad if not universal, its rise may be a factor in the E–T and σ–T jogs of $MgAl_2O_4$ noted earlier (at $\sim 500 - 700$ °C) [35], similar to, but less pronounced than, for ZrO_2. While the EA of MgO [130–132] is relatively low at 22 °C, hence much less likely to be a factor at moderate temperature, its substantial EA levels at higher temperature [132], e.g. $\sim$1200 °C, may be related to increased fracture initiation from even relatively clean (i.e. recrystallized) grain boundaries at $> \sim$1200 °C [55, 57]. Thus, EA needs to be considered as another broad factor besides, or in addition to grain boundary impurities in increasing intergranular failure with increasing temperature.

Other materials show little or no initial strength decrease until temperatures of $\sim$1000 °C or higher. Thus, ThO_2 and UO_2 show higher strength at 1000 versus 22 °C (Figs 7 and 8). Whether such effects in ThO_2 are related to mechanical and electrical relaxation in the temperature range is unknown. Further, as noted earlier, non-oxides such as B_4C, SiC and TiC show limited, or possibly, no initial strength decrease, in some cases possibly a slight increase with initial temperature increases, in contrast to the E–T decrease (typically a few to $\sim$10% to 1000 °C). Some of these differences could reflect reduction of TEA stresses, e.g. in B_4C, but in the case of B_4C, effects of substantial

twinning, and in α-SiC of polytypes, are unknown. While oxidation may also be a factor, tests in neutral or reducing atmospheres show this is, at best, a partial factor.

3.5. Overall mechanisms

The changes in strength with temperature, environment, and grain size are overall consistent with flaw-induced failure. Thus, SCG is a well established adjunct to normal flaw failure, and microplastic nucleation of cracks, or assisting their growth are accepted mechanisms interacting, and consistent, with conventional flaw failure. The same is true of changes in single crystal strengths and changes in grain boundary effects whether intrinsic, e.g. due to changes in TEA or EA stresses, or extrinsic, e.g. due to impurities. However, while the above concepts are known, fully effective quantification of the contributions to failure are often not feasible.

The situation is far more uncertain for reconciling the reviewed strength changes with bridging, which has been widely cited as an important factor in the strength behaviour of many ceramics considered here, e.g. Al_2O_3 [134]. There are basic, generic issues concerning the applicability of bridging to normal strength behaviour [135, 136] which are beyond the scope of this paper. However, the current attention to bridging and the general increase of bridging with increased intergranular fracture, which is often much greater with slow crack growth, and typical increases with test temperature [136], make some comments on its applicability to the observations of this paper in order. Bridging is normally observed after the fact, i.e. with an arrested crack, *in situ* in a scanning electron microscope (SEM), so possible effects of SCG on it are not observed. The frequent occurrence of SCG via intergranular fracture, which favours bridging, would imply that the toughening due to bridging should limit the reduction of strength from SCG, e.g. to substantially less than in single crystals (if the latter occurs), but there is no clear evidence of this, e.g. in Al_2O_3.

Equally, or more, serious questions arise with the changes in strength with increasing temperature. Thus, the strength minima and maxima observed with sapphire, as well as a number of (mainly larger-grained) polycrystalline Al_2O_3 bodies, raises questions of how a single crystal mechanism, e.g. possibly twinning in sapphire noted earlier, impact a polycrystalline body. Clearly, this can be the case if flaws causing failure are on the scale of one or a few grains as indicated earlier, but it seems unlikely that twinning could impact failure with flaw propagation over several to many grains as implied by crack scales needed for bridging, as also implied by the absence of strength minima and maxima in finer-grained Al_2O_3 bodies where cracks cover a number of grains. Again, the increased intergranular fracture with increased temperature over much of this range also raises questions about bridging in view of the strength decreases that occur.

The behaviour of other materials also raises serious question regarding the role, if any, of bridging on their normal strength behaviour. Thus, BeO generally shows the opposite strength–temperature trend to $\sim$1000 °C, but has similar Young's modulus, TEA, and SCG to Al_2O_3, so at least one of these two materials would appear to not be consistent with bridging. MgO shows similar, though more moderate, trends than BeO, but not greatly less as would be expected if TEA stresses (absent in MgO) were a major factor in bridging, as commonly proposed. ZrO_2 shows substantial strength decrease with initial temperature increases, which is accompanied by some increase in intergranular failure, which should aid bridging, and hence limit strength decrease, i.e. the opposite of what appears to happen. Also, the decrease in Young's modulus, which appears to be due to lattice defects, raise further questions of how bridging could be a factor in strength changes.

4. Summary and conclusions

Evaluation of σ–$G^{-1/2}$ behaviour from -200 to $\sim$1300 °C shows this typically follows a two-branched behaviour as at 22 °C; i.e. limited grain size dependence at finer grain size due to $C < G$, and a substantial grain size dependence at larger grain size due to $C \leqslant G$. Such two-branched behaviour reinforces the dominance of flaw mechanisms of failure. Where microplastic failure occurs, mainly at medium and larger grain size, strength approximately extrapolates to the stress for the easiest activated mode of single crystal microplasticity. Higher relative strengths of materials such as ThO_2 and UO_2 at higher temperature may indicate increasing effects of microplasticity. Where flaw failure occurs, strengths at large grain size generally extend well below strengths for the weakest crystal orientation. No clear differentiation between cubic and non-cubic materials failing from flaws was found; i.e. the mechanisms of failure are not primarily determined by structurally related effects. There is some indication of non-oxide (i.e., more covalently bonded) materials having higher relative strength. However, if so, it is not clear whether it is intrinsic or simply due to more successful development. Much remains to be documented and understood of such overall σ–G–T behaviour.

While flaw failure predominates, substantial complexity exists as reflected in significant deviations, especially from E–T behaviour. Shifts in single- versus poly-crystal strengths and possibly between strengths for different grain sizes occur due to SCG and other effects, mainly at $\leqslant$ 1000 °C, where testing is often neglected (other than at 22 °C and -196 °C). SCG effects (due to H_2O) on σ occur only during external stressing, apparently either not occurring, or (more probably) fairly rapidly saturating due to internal (e.g. TEA) stresses alone. SCG does not occur in all crystals (e.g. CaO, MgO, ZrO_2 and probably not in MgF_2, ZnSe, AlN or Si_3N_4). However, SCG can occur intergranularly in polycrystalline bodies of at least some of these materials, e.g. due to grain boundary phases having known or suspected SCG. SCG is effected by temperature, and may be interactive with

microplasticity, TEA and EA, and surface machining stresses. Sapphire strength drops rapidly from at least $-196\,^{\circ}C$ to a minimum at ~ 400–$800\,^{\circ}C$, then rises to a maximum at 900–1100 °C, before steadily decreasing at higher temperature. Polycrystalline Al_2O_3 often shows a similar, though usually less drastic initial strength drop, and may exhibit: (1) a strength minimum, a subsequent maximum (similar to, but less extreme than for single crystals), or both; or (2) an approximate strength plateau at intermediate temperature (e.g. 400–800 °C). Both of these trends appear to require sufficiently large grains and be overridden by the presence of other sources of failure, e.g. pores. Both are also in contrast to the simple, steady, moderate decrease of Young's modulus (e.g. ~ 10–15% by 1200 °C) which would also be the expected strength trend if only simple flaw failure were occurring. In contrast to this BeO crystals show similar, simple σ–T and E–T trends. Polycrystalline BeO also does not show the rapid initial strength drop at $> 22\,^{\circ}C$ that Al_2O_3 does, but often shows significant strength maxima at intermediate temperature, with impurities (or additives) again limiting these. MgO, while showing overall σ–T dependence consistent with slip-induced fracture, shows intermediate temperature polycrystalline strength maxima (less pronounced than in BeO) or plateaus similar to BeO and Al_2O_3. ZrO_2 shows polycrystalline E decreasing more rapidly with increasing temperature than single crystal Young's moduli, and even greater strength decreases. Other more limited oxide and non-oxide data indicates some strength increases, or no decrease from 22 to $\sim 1000\,^{\circ}C$ (including in non-air atmospheres, ruling out surface oxidation effects), i.e. not following E–T decreases nor those expected due to relaxation of surface machining stresses.

A tentative sorting of some of the above complexities is as follows. The rapid sapphire strength drop with increasing temperature may reflect failure from crack–twin combinations (which are probably also susceptible to H_2O SCG and grain size effects). The subsequent strength maxima in Al_2O_3 (and BeO) may reflect increased microplasticity to allow crack tip blunting in sapphire, but probably reflects more reduction in TEA in polycrystals, especially in fine grain bodies (e.g. fibres) due to less opportunity for such microplastic crack blunting there. Grain boundary, e.g. SiO_2-based, phases further favour TEA reduction, but can also over-ride such effects due to grain boundary sliding (but varies with processing dependent boundary wetting by such phases). Transformation may be a factor in more rapid initial E–T and especially σ–T ZrO_2 decreases, but only in partially stabilized ZrO_2. H_2O–Y_2O_3 corrosion, SCG, or both effects may also be a factor, but only over a limited composition and temperature range. Both EA and grain boundary impurities are probably also factors in reduced strength and increased intergranular fracture, especially at higher temperature. E–T and hence σ–T ZrO_2 decreases correlate with lattice defect (and related internal friction) effects which probably extend to several other materials, e.g. CeO_2, ThO_2, UO_2 and $MgAl_2O_4$. Thus, while the above factors probably alter, but are consistent with flaw failure, giving insight to the observed trends, consideration of crack bridging do not. In fact, most of the observed trends seriously question whether bridging is a factor in most normal strength behaviour.

While existing data provides some insight, a great lack of information is revealed. Not only is there very little SCG information on single crystals (including materials for which crystals are readily available, e.g. TiO_2 and $MgAl_2O_4$), but the documentation in the most studied material, sapphire, is incomplete. Data for grain size effects in polycrystalline materials are even less well defined. While there is reasonable evidence of TEA effecting strength, specifics of this are still lacking, e.g. levels of these stresses, and how their effects depend on key parameters, e.g. flaw size. While significant EA increases with temperature may cause increased grain boundary fracture initiation of many ceramics at higher temperatures, much less is known of its effects. Besides direct studies, this also requires more single crystal elastic moduli–temperature data. Finally, an overall key need is for polycrystalline studies that explore enough variables, e.g. grain size, temperature, elastic moduli and strength, that provide a reasonable opportunity of sorting out different factors. Narrow studies, focused on a single, often simplistic, approach or mechanism are of much less, if any, use.

Acknowledgements

Dr R. Ruh of the Air Force Materials Laboratory (now retired) is thanked for comments on the manuscript.

References

1. R. W. RICE, *J. Mater. Sci.* in press.
2. *Idem.*, in "Fracture mechanics and ceramics", Vol. 1, edited by R. C. Bradt, D. P. H. Hasselman and F. F. Lange (Plenum Press, New York, 1974) p. 323.
3. *Idem.*, in "Treatise on materials science and technology, Properties and Microstructure", Vol. 11, edited by R.-C. McCrone, (Academic Press, New York, 1977) p. 199.
4. *Idem.*, in "The science of ceramic machining and surface finishing II", National Bureau of Standards Special Publication 562, edited by B. J. Hockey and R. W. Rice (US Government Printing Office, Washington, DC 1979).
5. H. NEUBER and A. WIMMER, AFML-TR-68-23 (1968).
6. R. W. DAVIDGE and G. TAPPIN, *Proc. Brit. Ceram. Soc.* **15** (1970) 47.
7. Reports of the AVCO Corp., Lowell, Mass., on "Microstructure Studies of Polycrystalline Refractory Oxides", for U.S. Naval Air Systems Command contracts, 1966–1968, edited by W. H. Rhodes, D. J. Sellers, R. M. Cannon, A. H. Heuer, W. R. Mitchell, and P. Burnett, Summary report AVSSD-0098-68-RR for Contract N000-19-67-C-0336 (1968).
8. R. W. RICE, *Proc. Brit. Ceram. Soc.* **20** (1972) 205.
9. W. B. CRANDALL, D. H. CHUNG and T. J. GRAY, in "Mechanical properties of engineering ceramics", edited by W. W. Kriegel and H. Palmour III (Wiley Interscience, New York, 1961) p. 349.
10. G. DEWITH, *J. Mater. Sci.* **19** (1984) 2195.
11. A. H. HEUER and J. P. ROBERTS, *Proc. Brit. Ceram. Soc.* **6** (1966) 17.
12. R. W. RICE, in Ceramic for High Performance Proceedings of 2nd Army Materials Technology, edited by J. J. Burke, A. E. Gorum and R. N. Katz (Brook Hill, Chestnut Hill, MA, 1974) p. 287.

13. J. B. WACHTMAN, Jr., and L. H. MAXWELL, *J. Amer. Ceram. Soc.* **42** (1959) 432.
14. J. CONGLETON, N. J. PETCH and S. A. SHIELS, *Phil. Mag.* **19** (1969) 795.
15. R. J. CHARLES, in "Studies of the brittle behavior of ceramic materials", Technical Report No. ASD-TR-628, 370–404, Aeronautical Systems Division, Wright Patterson AFG, Ohio (1962).
16. R. M. GRUVER, W. A. SOTTER and H. P. KIRCHNER, "Fractography of Ceramics", Summary Report, Naval Air Systems Command, Report for Contract No. N00019-73-C-0356, Nov. 22, 1974.
17. C. C. McMAHON, *Amer. Ceram. Soc. Bull.* **58** (1979) 873.
18. S. L. DOLE, O. HUNTER, Jr., F. W. CALDERWOOD and D. J. BRAY, *J. Amer. Ceram. Soc.* **61**(11–12) (1978) 486.
19. E. A. JACKMAN and J. P. ROBERTS, *Trans. Brit. Ceram. Soc.* **54** (1955) 389.
20. P. SHAHINIAN, *J. Amer. Ceram. Soc.* **54** (1971) 67.
21. S. M. WIEDERHORN, B. J. HOCKEY and D. E. ROBERTS, *Phil. Mag.* **28** (1973) 783.
22. G. F. HURLEY, *Appl. Polym. Symp.* **21** (1976) 121.
23. M. IWASA and R. C. BRADT, in "Advances in ceramics, Vol. 10, Structure and properties of MgO and Al_2O_3 ceramics" edited by W. D. Kingery (American Ceramic Society, Columbus, OH, 1984) p. 767.
24. H. SAYIR, K. P. D. LAGERTOF, M. R. DeGUIRE and A. SAYIR, 16th Annual Conference and Exposition on Composites and Advanced Ceramics, Cocoa Beach, Florida, January 7–10, 1991.
25. S. C. CARNIGLIA, *J. Amer. Ceram. Soc.* **48** (1965) 580.
26. *Idem.*, *ibid.* **55** (1972) 243.
27. H. P. KIRCHNER, *Mater. Sci. Engng* **13** (1974) 63.
28. *Idem.*, "Strengthening of ceramics, treatments, tests and design applications" (Marcel Dekker, Inc., NY, 1979) p. 88.
29. H. MIZUTA, K. ODA, Y. SHIBASAKI, M. MAEDA, M. MACHIDA and K. OSHIMA, *J. Amer. Ceram. Soc.* **75** (1992) 469.
30. J. R. McLAREN and R. W. DAVIDGE, *Proc. Brit. Ceram. Soc.* **25** (1975) 151.
31. N. M. PARIKH, in "Nuclear applications of nonfissionable ceramics", edited by A. Boltax and J. H. Handwerk (American Nuclear Soc., Hindsdale, IL., 1966) p. 31.
32. R. M. SPRIGGS and T. VASILOS, *J. Amer. Ceram. Soc.* **46** (1963) 224.
33. R. M. SPRIGGS, J. B. MITCHELL and T. VASILOS, *ibid.* **47** (1964) 323.
34. G. ORANGE, D. TURPIN-LAUNAY, P. GOEURIOT, G. FANTOZZI and F. THEVENOT, *Sci. of Ceram.* **12** (1984) 661.
35. J. C. ROMINE, *Cer. Eng. Sci. Proc.* **8** (1987) 755.
36. M. H. STACEY, *Brit. Ceram. Trans.* **87** (1977) 168.
37. J. E. BAILEY and H. A. HILL, "Ceramic fibers for the reinforcement of gas turbine blades", edited by W. W. Kreigel and H. Palmour, III. (Plenum Press, NY, 1971) p. 341.
38. J. B. WACHTMAN, Jr., W. E. TEFFT, D. G. LAM, Jr., and C. S. APSTEIN, *Phys. Rev.* **122** (1961) 1754.
39. J. B. WACHTMAN, Jr. and D. G. LAM Jr., *J. Amer. Ceram. Soc.* **42** (1959) 254.
40. R. DUFF and P. BURNETT, "Microstructure studies of polycrystalline refractory oxides", Summary Report for Contract No. 3-65-0316-f (1966).
41. G. G. BENTLE and R. M. KNIEFEL, *J. Amer. Ceram. Soc.* **48** (1965) 570.
42. W. B. ROTSEY, K. VEEVERS and N. R. McDONALD, *Proc. Brit. Cer. Soc.* **7** (1967) 205.
43. G. G. BENTLE and K. T. MILLER, *J. Appl. Phys.* **38** (1967) 4248.
44. B. A. CHANDLER, E. C. DUDERSTADT and J. F. WHITE, *J. Nucl. Mater.* **8** (1963) 329.
45. R. E. FRYXELL and B. A. CHANDLER, *J. Amer. Ceram. Soc.* **47** (1964) 283.
46. M. L. STEHSEL, R. M. HALE and C. E. WALLER, in "Mechanical Properties of Engineering Ceramics", edited by W. Kriegel and H. Palmour III (Wiley Interscience, New York, 1961) p. 16.
47. S. C. CARNIGLIA, R. E. JOHNSON, A. C. HOTT and G. G. BENTLE, *J. Nucl. Mater.* **14** (1964) 378.
48. D. A. SHOCKEY and G. W. GROVES, *J. Amer. Ceram. Soc.* **51** (1968) 299.
49. K. R. JANOWSKI and R. C. ROSSI, *ibid.* **51** (1968) 453.
50. R. W. RICE, *ibid.* **52** (1969) 428.
51. S. M. COPLEY and J. A. PASK, *ibid.* **48** (1965) 139.
52. D. S. THOMPSON and J. P. ROBERTS, *J. Appl. Phys.* **31**(2) (1960) 433.
53. W. H. RHODES, R. M. CANNON, Jr. and T. VASILOS, in "Fracture machanics of ceramics", edited by R. C. Bradt, D. P. H. Hasselman and F. F. Lange (Plenum Press, NY, 1973) p. 709.
54. R. W. RICE, *Proc. Brit. Ceram. Soc.* **20** (1972) 329.
55. A. G. EVANS, D. GILLING and R. W. DAVIDGE, *J. Mater. Sci.* **5** (1970) 187.
56. R. W. RICE, *J. Amer. Ceram. Soc.* **55** (1972) 90.
57. *Idem.*, *ibid.* **76** (1993) 3009.
58. R. B. DAY and R. J. STOKES, *J. Amer. Ceram. Soc.* **49** (1966) 345.
59. T. N. ASILOR, J. B. MITCHELL and R. M. SPUGGS, *J. Amer. Ceram. Soc.* **47** (1964) 606.
60. F. P. KNUDSEN, *J. Amer. Ceram. Soc.* **42** (1959) 376.
61. C. E. CURTIS and J. R. JOHNSON, *ibid.* **40** (1957) 63.
62. M. D. BURDICK and H. S. PARKER, *J. Amer. Ceram. Soc.* **39** (1956) 181.
63. F. P. KNUDSEN, H. S. PARKER and M. D. BURDICK, *ibid.* **43** (1960) 641.
64. A. G. EVANS and R. W. DAVIDGE, *J. Nucl. Mater.* **33** (1969) 249.
65. R. J. BEALS, J. H. HANDWERK and G. M. DRAGEL, in High Temperature Technology, Proceedings of the Third International Symposium on High Temperature Technology, Pacific Grove, CA (International Union of Pure & Applied Chemistry, Butterworths, London, 1968) p. 265.
66. R. F. CANON, J. T. A. ROBERTS and R. J. BEALS, *J. Amer. Ceram. Soc.* **54** (1971) 105.
67. C. R. KENNEDY and G. BANDYOPADHYAY, *ibid.* **59** (1976) 176.
68. H. M. KANDIL, J. D. GREINER and J. F. SMITH, *ibid.* **67** (1984) 341.
69. J. B. WACHTMAN, Jr. and W. C. CORWIN, *J. Res. National Bureau of Standards – A. Physics and Chemistry* **69A** (1965) 457.
70. M. SHIMADA, D. MATSUSHITA, S. KURATANI, T. OKAMOTO, M. KOIZUMI, K. TSUKUMA and T. TSUKIDATE, *J. Amer. Ceram. Soc.* **67** (1984) C23.
71. J. W. ADAMS, D. C. LARSEN, R. RUH and K. S. MAZDIYASMI, *J. Amer. Ceram. Soc.* in press.
72. S. L. DOLE, *Commun. Amer. Ceram. Soc.* **66** (1983) C47.
73. M. WELLER and H. SCHUBERT, *J. Amer. Ceram. Soc.* **69** (1986) 573.
74. M. OZAWA, T. HATANAKA and H. HASEGAWA, *J. Ceram. Soc. Japan* **99** (1991) 628.
75. K. NISHIYAMA, M. YAMANAKA, M. OMORI and S. UMEKAWA, *J. Mater. Sci. Lett.* **9** (1990) 526.
76. S. L. DOLE, O. HUNTER, Jr. and F. W. CALDERWOOD, *J. Amer. Ceram. Soc.* **63** (1980) 136.
77. R. P. INGEL, D. LEWIS, B. A. BENDER and R.W. RICE, *ibid.* **65** (1982) C150.
78. A. S. DRACHINSKII, V. A. DUBOK, V. V. LASHNEVA, V. G. VERESHCHAK and V. V. KOVYLYAEV, *Problemy Prochnosti* **3** (1988) 77, (1987) 368, translated.
79. R. W. RICE, in "Fractography of ceramic and metal failure", edited by J. J. Mecholosky Jr. and S. R. Powell (ASTM STP 827, 1984) p. 5.
80. Y. MAEHARA and T. G. LANGDON, *J. Mater. Sci.* **25** (1990) 2275.
81. R. L. STEWART and R. C. BRADT, *ibid.* **15** (1980) 67.
82. R. L. STEWART and R. C. BRADT, *J. Amer. Ceram. Soc.* **63** (1980) 619.
83. A. GHOSH, K. W. WHITE, M. G. JENKINS, A. S. KOBAYASHI and R. C. BRADT, *J. Amer. Ceram. Soc.* **74** (1991) 1624.

84. R. A. ALLIEGRO, in "The encyclopedia of electrochemistry", edited by C. Hampell (Reinhold Pub. Corp. NY, 1964) p. 1125.
85. D. KALISH, E. V. CLOUGHERTY and K. KREDER, *J. Amer. Ceram. Soc.* **52** (1969) 30.
86. H. R. BAUMGARTNER and R. A. STEIGER, *ibid.* **67** (1984) 207.
87. YUKIO TAKEDA and KUNIHIRO MAEDA, *J. Ceram. Soc. Japan* **99** (1991) 699.
88. D. C. LARSEN, J. W. ADAMS, L. R. JOHNSON, A. P. S. TEOTIA and L. G. HILL, "Ceramic materials for advanced heat engines, technical and economic evaluation" (Noyes Pub., Park Ridge, NJ, 1985).
89. G. DeWITH, *J. Mater. Sci.* **19** (1984) 457.
90. M. BOUGOIN, F. THEVENOT, J. DUBOIS and G. FANTOZZI, *J. Less-Common. Metals* **114** (1985) 257.
91. G. A. GOGOSTI, Y. A. L. GROUSHEVSKY, O. B. DASHEVSKAYA, Y. U. G. GOGOTSI and V. A. LAVRENKO, *ibid.* **117** (1986) 225.
92. G. W. HOLLENBERG and G. WALTHER, *J. Amer. Ceram. Soc.* **63** (1980) 610.
93. D. B. MIRACLE and H. A. LIPSITT, *ibid.* **66** (1983) 592.
94. R. H. J. HANNINK and M. J. MURRAY, *J. Mater. Sci.* **9** (1974) 23.
95. J. J. GILMAN, in Fracture, Proceedings of the International Conference on Atomic Mechanisms of Fracture edited by B. Averbach, D. Felbeck, G. Hahn and D. Thomas (John Wiley & Sons, New York, 1959) p. 193.
96. J. J. MECHOLSKY JUN, S. W. FREIMAN and R. W. RICE, *J. Mater. Sci.* **11** (1976) 1310.
97. B. E. WALKER, Jr., R. W. RICE, R. C. POHANKA and J. R. SPANN, *Amer. Ceram. Soc. Bull.* **55** (1976) 274.
98. J. P. SINGH, A. V. KEKAR, D. K. SHETTY and R. S. GORDON, *J. Amer. Ceram. Soc.* **62** (1979) 179.
99. A. G. EVANS, *ibid.* **63** (1980) 115.
100. A. V. VIRKAR, D. K. SHETTY and A. G. EVANS, *ibid.* **64** (1981) 56.
101. H. P. KIRCHNER and J. M. RAGOSTA, *ibid.* **63** (1980) 490.
102. R. W. RICE, *ibid.* **76** (1993) 1068.
103. S. W. FREIMAN, *Ceram. Int.* **2** (1976) 111.
104. E. K. BEAUCHAMP and S. L. MONROE, *J. Amer. Ceram. Soc.* **72** (1984) 1179.
105. A. FORT, D. SHARP, B. ASH, K. PAPWORTH and D. REED, *ibid.* **55** (1972) 329.
106. K. R. McKINNEY, B. A. BENDER, R. W. RICE and C. CM. WU, Jr., *J. Mater. Sci.* **26** (1991) 6467.
107. M. E. O'DAY and G. L. LEATHERMAN, *Int. J. Microcircuits & Elect. Pack.* **16** (1993) 41.
108. L. E. DOLHERT, J. H. ENLOE, R. W. RICE, C. CM. WU, K. McKENNIG, S. W. FREEMAN and G. S. WHITE, in preparation.
109. R. W. RICE and C. C. WU, in preparation.
110. A. H. HEUER, *Phil. Mag.* **13** (1966) 379.
111. P. F. BECHER, *J. Amer. Ceram. Soc.* **59** (1976) 143.
112. *Idem., ibid.* **59** (1976) 59.
113. W. D. SCOTT and K. K. ORR, *ibid.* **66** (1983) 27.
114. H. M. CHAN and B. R. LAWN, *ibid.* **7** (1988) 29.
115. B. E. WALKER, Jr., R. W. RICE, R. C. POHANKA and J. R. SPANN, *Amer. Ceram. Soc. Bull.* **55** (1976) 274.
116. R. W. RICE and R. C. POHANKA, *J. Amer. Ceram. Soc.* **62** (1979) 559.
117. R. W. RICE, R. C. POHANKA and W. J. McDONOUGH, *ibid.* **63** (1980) 703.
118. R. W. RICE, in "Fractography of glasses and ceramics II", Ceramic Transactions, Vol. 17, edited by J. R. Varner and V. D. Frechette (American Ceramics Society, Westerville, OH, 1991) p. 509.
119. R. W. RICE, S. W. FREIMAN and P. F. BECHER, *J. Amer. Ceram. Soc.* **64** (1981) 345.
120. F. J. P. CLARKE, *Acta Metall.* **12** (1964) 139.
121. M. K. AGHAJANIAN, N. H. MACMILLAN, C. R. KENNEDY, S. J. LUSZCZ and R. ROY, *J. Mater. Sci.* **24** (1989) 658.
122. J. S. MOYA, R. MORENO and J. REQUENA, *J. Amer. Ceram. Soc.* **71** (1988) C479.
123. R. W. RICE, *J. Amer. Ceram. Soc.* **75** (1991) 1745.
124. J. B. WACHTMAN, Jr., *Phys. Rev.* **131** (1963) 517.
125. J. J. SWAB, *J. Mater. Sci.* **26** (1991) 6706.
126. M. HIRANO, T. MATSUYAMA, H. INADA, K. SUZUKI, H. YOSHIDA and M. MACHIDA, *J. Ceram. Soc. Japan* **99** (1991) 382.
127. I. THOMPSON and R. D. RAWLINGS, *J. Mater. Sci.* **27** (1992) 2823.
128. *Idem., ibid.* **27** (1992) 2831.
129. T. QUADIR and W. R. GRACE, private communication, 1991.
130. D. H. CHUNG and W. R. BUESSEM, in Proceedings international symposium, Vol. 2, edited by F. W. Vahldiek and S. A. Mersol (Plenum Press, NY, 1968) p. 217.
131. G. SIMMONS and H. WANG, "Single crystal elastic constants and calculated aggregate properties: a handbook" (The MIT Press, Cambridge, MA, London, UK, 1977).
132. R. W. RICE, *J. Mater. Sci. Lett.* **13** (1994) 1261.
133. R. W. RICE, C. Cm. WU and F. BORCHELT, *ibid.* **77** (1994) 2539.
134. P. CHANTIKUL, S. J. BENNISON and B. R. LAWN, *ibid.* **73** (1990) 2419.
135. R. W. RICE, *ibid.* **76** (1993) 1898.
136. *Idem.* in "Fractography of glasses and ceramics III", edited by V. Frechette, J. R. Varner and G. Quinn (American Ceramics Society, Westerville, OH, 1996) p. 1.

Received 18 March
and accepted 4 November 1996